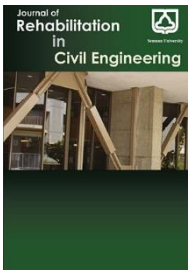

Journal homepage: http://civiljournal.semnan.ac.ir/

In-Plane Cyclic Response of Separated Masonry Infill Walls Using Polymeric Materials at the Surrounding Steel Frames Interface Using 3D FE Analysis

Alireza Karkabadi[1], Mohammad Iman Khodakarami[2*]

1. M.Sc. Student, Faculty of Civil Engineering, Semnan University, Semnan, Iran
2. Associate Professor, Faculty of Civil Engineering, Semnan University, Semnan, Iran
Corresponding author: *Khodakarami@semnan.ac.ir*

ARTICLE INFO

Article history:
Received: 24 January 2022
Revised: 24 September 2022
Accepted: 27 September 2022

Keywords:
Seismic isolation;
Polymeric materials;
Masonry walls;
In-plane cyclic loading;
Steel frame.

ABSTRACT

Masonry infill walls are commonly used as partitions and exterior walls in many countries. Generally, the masonry wall is executed without any gap from the frame, which leads to the interaction between the structural frame and the infill wall. Interaction between the structural frame and the masonry infill wall can damage the frame and the infill wall. Therefore, it is necessary to find a solution to improve the performance of masonry infill walls in the structural frame. Isolation of the masonry infill wall from the surrounding frame by polymeric material is the idea of this paper to decrease the damage to the structure and masonry infill. In this essay, Finite element models of steel infill frame and isolated infill frame subjected to In-Plane cyclic loading are developed in ABAQUS. For this purpose, three one-bay, one-story masonry-infilled steel frames with different frame ratios of height to the length (H/B) isolated by different polymeric materials with various thicknesses were investigated. Isolation of masonry infill can reduce the base reaction about 25%. In the Isolated Infill wall, the drift's amount increases about two times compared with the unseparated infill wall. Therefore, it damages the masonry infills up to moderate drifts, while full interaction is still in place drifts are large. Also, infill walls isolated by a softer polymer, have better performance. In brief, isolation of infill wall using polymeric materials improves the behavior of the infill and frame.

1. Introduction

In most design codes, as a usual assumption, masonry infill panels are considered nonstructural elements. Masonry infill walls are commonly used as partitions and exterior walls as the primary goal. Generally, a

How to cite this article:
Karkabadi, A., & Khodakarami, M. I. (2023). In-Plane Cyclic Response of Separated Masonry Infill Walls Using Polymeric Materials at the Surrounding Steel Frames Interface Using 3D FE Analysis. *Journal of Rehabilitation in Civil Engineering*, *11*(3), 18-46. https://doi.org/10.22075/JRCE.2022.26037.1602

masonry infill wall is built without any gap from the structural frame. So, the interaction between the masonry infill wall and the surrounding frame affects the overall performance of the structure[1-2]. Often and not always, the interaction of the masonry infill with the surrounding frame has an adverse effect on the overall performance of the structure[3]. Because the infill wall has a high contribution to the Lateral stiffness and strength of the structure. In that case, the infills may invalidate the structure's seismic design and challenge design codes' intention to control the inelastic response, as shown in past earthquake reports. Also, the aftershocks in the seismic sequence have a unique effect on infill walls[4]. The brittle behavior and low tensile strength of masonry infill panels can be a reason of damage to the structure during an earthquake. in[5]the development of fragility curves for brick infill walls in steel frame structures was discussed. Seismic design codes expressed the negative effects of masonry infill wall on the performance of the structure as follows:

1. Due to the absence of the infills at the ground story, produce a soft story at the ground story.
2. Increasing the inelastic deformation demands in the part of the building with more-sparse infills due to the non-uniformly distributed position of infills in the elevation or plan.
3. Brittle failure of frame members and the connections due to the interaction between the infill wall and the surrounding frame.

Nonstructural components (architecture, mechanical, electrical, plumbing, furniture, accessories, equipment) have higher costs than structural components [6,7]. Also, by damage to nonstructural elements, especially masonry infills during the earthquake, emergency evacuation of the building is disrupted. One of the methods to reduce the damage of masonry infill and the surrounding frame is the isolation of the masonry infill from the structural frame. Some studies [8-17] investigated the effects of separation of masonry infill using air gap.

Other methods with target:

1. The sliding mechanism occurs in the brick's layer in masonry infills to increase ductility and reduce lateral stiffness and strength [18-23].
2. Decreasing the infill stiffness and the damage by using softer masonry blocks at the point of interaction of the masonry wall with the frame [24].
3. Applying fuses or isolators as Energy attenuative devices in the perimeter of the infill [25-28]. Also, Masonry wall reinforcement
4. Using timber lumbers to improve the masonry infill performance [29].
5. Procuring a more deformable masonry using soft plastic joints as a connection between bricks [30].
6. invention and development of structurally favorable masonry units, which would strengthen beneficial aspects of steel-frame interaction and alleviate negative aspects[31].

Isolation of masonry infill from the surrounding frame using air gap, although it can improve masonry infill's in-plane performance, reduces the out-of-plane stability of masonry infill. Also, using an isolator device and fuse can be expensive and complicated.

A new concept in separating the masonry infill walls from the surrounding steel frame has been investigated [32]. At the interaction point of the masonry infill and the structural frame, the performance of the masonry infill is improved by placing a thin layer of polymeric material with high energy absorbing capacity and ductility[33] By doing this, at low drifts, the interaction between steel frames and masonry infill is reduced. Also, the infill steel frames act like bare frames. At high drifts, the polymeric material is highly compressed[33]. In this paper, three steel moment frames in different ratios of height to length (H/B) in various isolator materials in different thicknesses of the layer are developed. Polymeric materials have good potential to achieve high strains (close to 1.0) in compression mode. So, they are imagined as useful elements for isolating masonry walls from the surrounding frame.

2. Problem statement

In order to evaluate the behavior of the masonry infill wall separated by polymeric materials at the junction of the frame and the wall, three main models were investigated according to Fig 1. In this study, three one-bay, one-story masonry-infilled steel frames with different frame height to the length ratios (H/B) isolated by different polymeric materials in different thicknesses of the layer were considered.

Three various models based on these variables are studied as follows:

a) Structural frames without infill wall (Bare frames)

b) Structural frames with masonry infill wall (Infill walls)

c) Isolation Infill wall from the surrounding frame using polymeric material (Isolation Infill walls)

All specimens are subjected to cyclic load. The masonry infill's stiffness and ultimate strength were obtained from the force-displacement diagram. Finally, the behavior of the isolated infill wall is compared with the non-isolated infill wall. Thus, it can be found how much the polymeric materials can reduce the masonry infill frame's stiffness and strength.

3. Numerical simulation

A numerical simulation was performed in this study to compare the isolation infill wall's behavior with the Masonry infill wall and the bare frame in Abaqus software. Also, the effect of polymeric materials in isolation of masonry infill wall from the structural frame was studied.

3.1. Bare Frame

Three steel moment frames with different height to length ratios (H/B) equal to 0.5, 1.0, and 2.0 were examined to obtain the bare frame specifications. These three frames were designed based on the AISC [34], the dead load was considered 500 kg/m^2, and the

live load was assumed 200 $kg/^{m^2}$. The examined two-dimensional frames are the side frames of the three-dimensional square plan. The geometries of frames are given in Table 1, and the schematic configuration of all three frames is shown in Fig. 1a. The used steel grade is ST37. In order to define the cyclic behavior of steel, the plasticity material model has been used. Beams and columns modeled using the C2D4R element. Beams and columns connection simulated with tie element. The boundary restraint was made by defining the conditions at column connections.

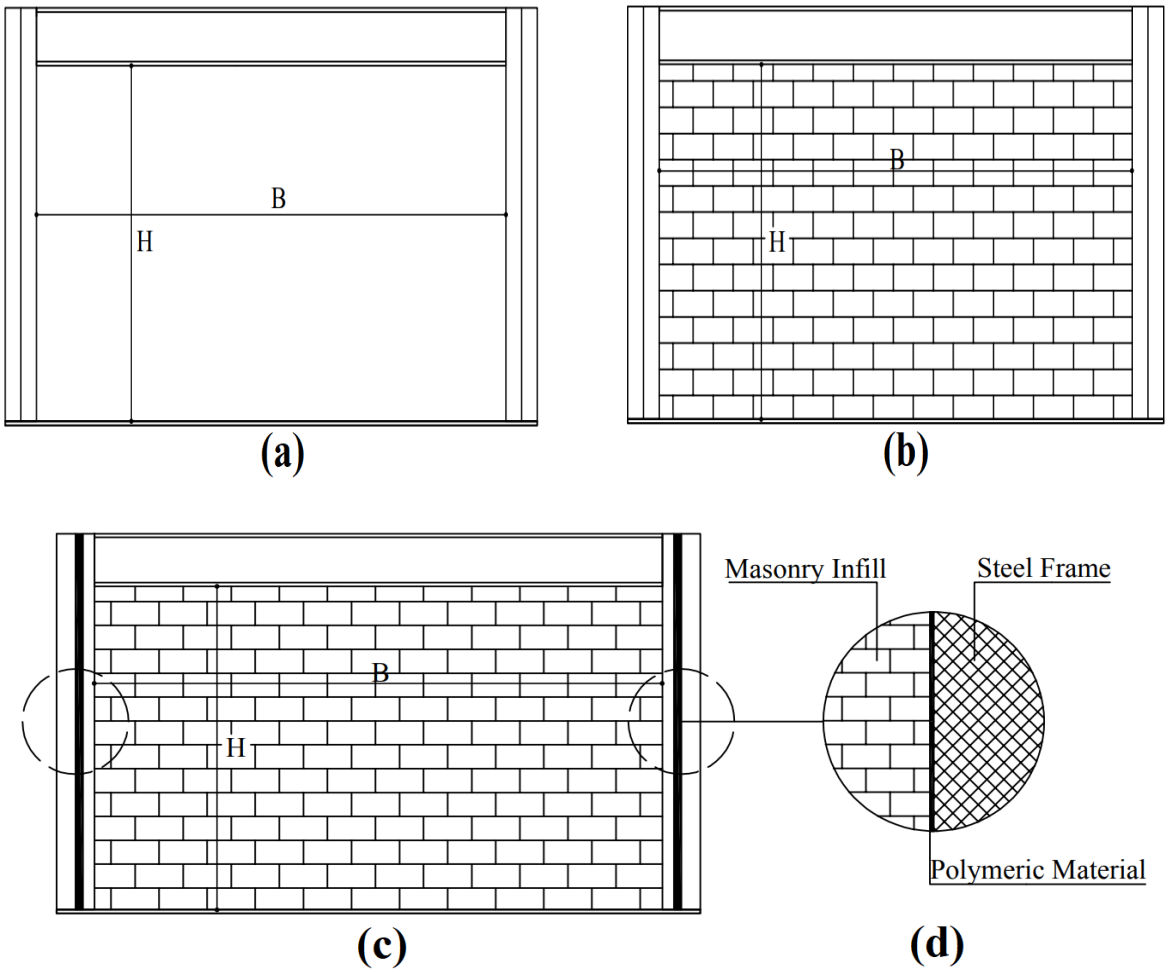

Fig. 1. Configuration of the three types of models: (a) Bare frame, (b) Infill wall, (c) Isolation infill wall, (d) Details of the isolation system.

Table 1. The geometry of considered frames (Bare Frames).

Models name	H/B	H(m)	B(m)	Beam Section	Column Section
BF-HB0.5	0.5	1.2	2.4	IPE160	IPE160
BF-HB1.0	1.0	1.2	1.2	IPE140	IPE140
BF-HB2.0	2.0	1.2	0.6	IPE120	IPE120

3.2. Masonry infill wall

Based on the three bare frames modeled in section 3.1, three masonry infill walls were modeled according to the geometric specifications of Table 2. The bricks (300x300x100 mm) and half-bricks (150x300x100 mm) are used to model the infill. Fig 2 shows the simulated bricks in the software. Also, the mechanical characteristics of the brick[35,36] to model the infill wall used in the software are given in Table 3. The masonry blocks were modeled with the C3D8R element. The angle of friction and mortar cohesion were supposed according to the engineering sentence due to the lack of data on the mortar type. The hard contact element with 44 degrees for the angle of friction and 0.5 for cohesion were considered for the mortar behavior simulation. The mortar contact element was used between the bricks layer and between bricks and the structural frame. The boundary conditions are similar to the section 3.1.

Table 2. The geometry of considered masonry infill frame (Infill Wall).

Models name	H/B	H(m)	B(m)	Tile in Length	Tile in Height
IW-HB0.5	0.5	1.2	2.4	8	4
IW-HB1.0	1.0	1.2	1.2	4	4
IW-HB2.0	2.0	1.2	0.6	2	4

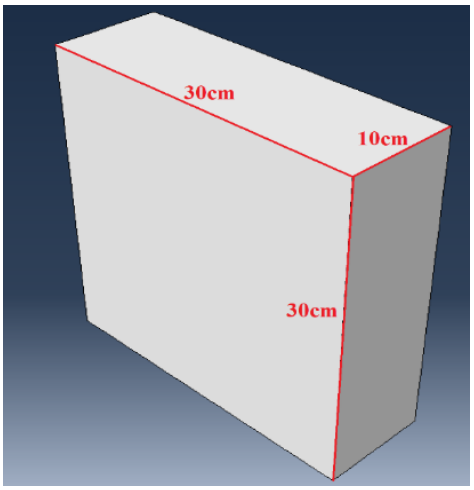

Fig. 2. The geometry of masonry Bricks Unit.

Table 3. Material characteristics of bricks [35-38].

Density ($^{kg}/_{m^3}$)	860	
Resilient modulus (GPa)	5.6	
Poisson ratio for masonry material	0.14	
Drucker Prager	Angel of Friction	44
	Flow Stress Ratio	1
	Dilation Angle	50

3.3. Isolation infill wall

In this part, the isolation masonry wall from the surrounding steel frame, simulated in Abaqus software with a micro modeling method. In this research, four different polymeric materials from [37-39], according to Table 4 mechanical properties, in four thicknesses of 5, 10, 15, and 20 mm were considered. The polymeric layers were modeled with a solid elastic element (C3D8R), and the polymer layer was placed at the connection of the column and the masonry wall. According to Fig. 3, the real stress-strain curve of polymeric materials is hyper-elastic (nonlinear-elastic), but in this paper, it was considered linear-elastic in order to simplification. The connection element of polymeric isolator and Masonry infill and frame is a mortar (hard contact element), as shown in Fig 1.d. The bare frame and masonry Infill frame modeling parameters are precisely the same as the previous sections. Table 5 shows the studied models in this section.

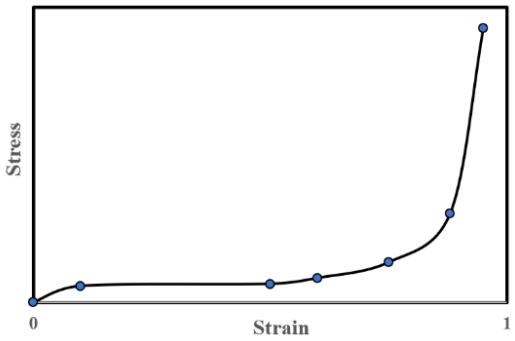

Fig. 3. Stress-strain curve of Polymeric materials.

Table 4. Mechanical properties of polymeric materials [37-39].

Material	Density (kg/m^3)	E (MPa)	□
Polyurethane (PU) [37]	38.2	3.3	0.3
Polystyrene (PS) [37]	19.5	2.24	0.3
Polyethylene (PE) [36]	80	3.9	0.3
Rubber (RU) [38]	1043	11.9	0.49

Table 5. Properties of the models with isolated infill walls.

		Models name			
Material	**H/B**	**Thickness of layer**			
		5	**10**	**15**	**20**
PU	**0.5**	ISO-HB0.5-PU5	ISO-HB0.5-PU10	ISO-HB0.5-PU15	ISO-HB0.5-PU20
	1.0	ISO-HB1.0-PU5	ISO-HB1.0-PU10	ISO-HB1.0-PU15	ISO-HB1.0-PU20
	2.0	ISO-HB2.0-PU5	ISO-HB2.0-PU10	ISO-HB2.0-PU15	ISO-HB2.0-PU20
PS	**0.5**	ISO-HB0.5-PS5	ISO-HB0.5-PS10	ISO-HB0.5-PS15	ISO-HB0.5-PS20
	1.0	ISO-HB1.0-PS5	ISO-HB1.0-PS10	ISO-HB1.0-PS15	ISO-HB1.0-PS20
	2.0	ISO-HB2.0-PS5	ISO-HB2.0-PS10	ISO-HB2.0-PS15	ISO-HB2.0-PS20
PE	**0.5**	ISO-HB0.5-PE5	ISO-HB0.5-PE10	ISO-HB0.5-PE15	ISO-HB0.5-PE20
	1.0	ISO-HB1.0-PE5	ISO-HB1.0-PE10	ISO-HB1.0-PE15	ISO-HB1.0-PE20
	2.0	ISO-HB2.0-PE5	ISO-HB2.0-PE10	ISO-HB2.0-PE15	ISO-HB2.0-PE20
RU	**0.5**	ISO-HB0.5-RU5	ISO-HB0.5-RU10	ISO-HB0.5-RU15	ISO-HB0.5-RU20
	1.0	ISO-HB1.0-RU5	ISO-HB1.0-RU10	ISO-HB1.0-RU15	ISO-HB1.0-RU20
	2.0	ISO-HB2.0-RU5	ISO-HB2.0-RU10	ISO-HB2.0-RU15	ISO-HB2.0-RU20

As shown in Fig. 4.b, at the corner of the frame, Cyclic Lateral Displacement (Fig. 4.a) was applied. Dynamic analysis was used to analyze the models in ABAQUS software.

3.4. Model verification

This paper used a numerical simulation in ABAQUS to verify the infill walls' behavior. For validation, the numerical modeling was compared with experimental results of [35]. A single-span one-story (the height to length ratio is equal to one) steel moment frame was tested by Flanagan and Bennett at the University of Tennessee, Knoxville, as shown in Fig. 5a. Also, according to Fig. 5b, numerical modeling of masonry frames was performed. The beam section is W310×52, and the column section is W310×52.

The masonry infill wall includes seven bricks in length and height. The dimensions of the infill are 2100 × 2100 mm. For modeling the infill wall, brick and half-brick were used. The brick unit's geometry was shown in Fig. 6 – and the characteristics of the used brick in the software were given in Table 3. In this experimental test, the loads were applied based on UBC 1991 features. The cyclic lateral displacement was imposed on the corner of the frame. Due to the lack of data, the friction angle and mortar cohesion were guessed according to the engineering judgment. The coefficient and angle of friction were assumed equal to (0.5-0.7) and (30-50), respectively [36]. Based on the sensitivity analysis, cohesion equal to 0.526 and degrees for friction angle equal to 42 were assumed. These values are close to the test results by [40]. In order to simulation of the behavior of mortar, C2D4R element was used for modeling the structural section of the frame. Beams and columns connection simulated with tie element. Fully fixed boundary conditions for displacements and rotations were applied at the bottom of the columns. The characteristics of the material were given in Table 6 based on [35,36].

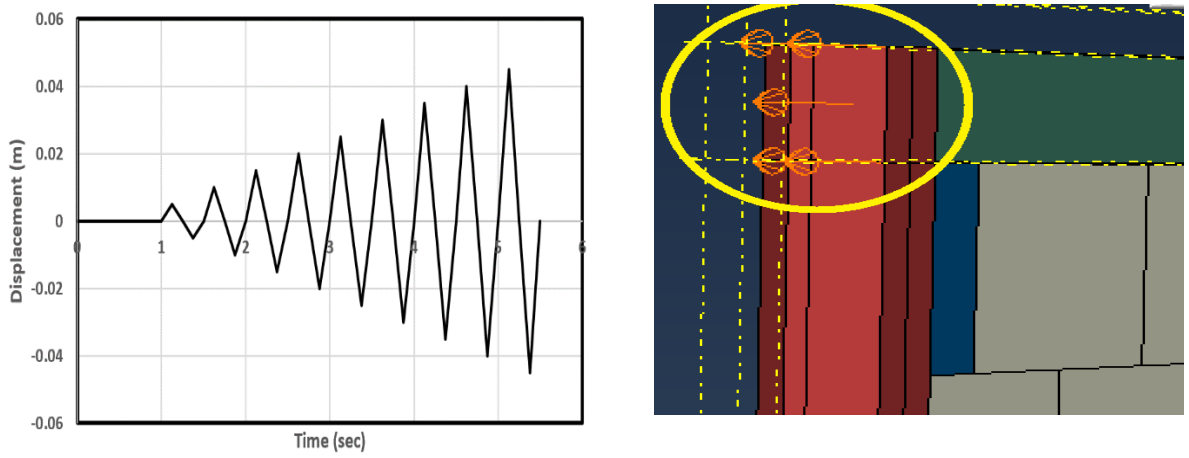

(a) **(b)**

Fig. 4. Simulation of Cyclic Loading protocol: (a) Displacement history; (b) Displacement Applied to frame.

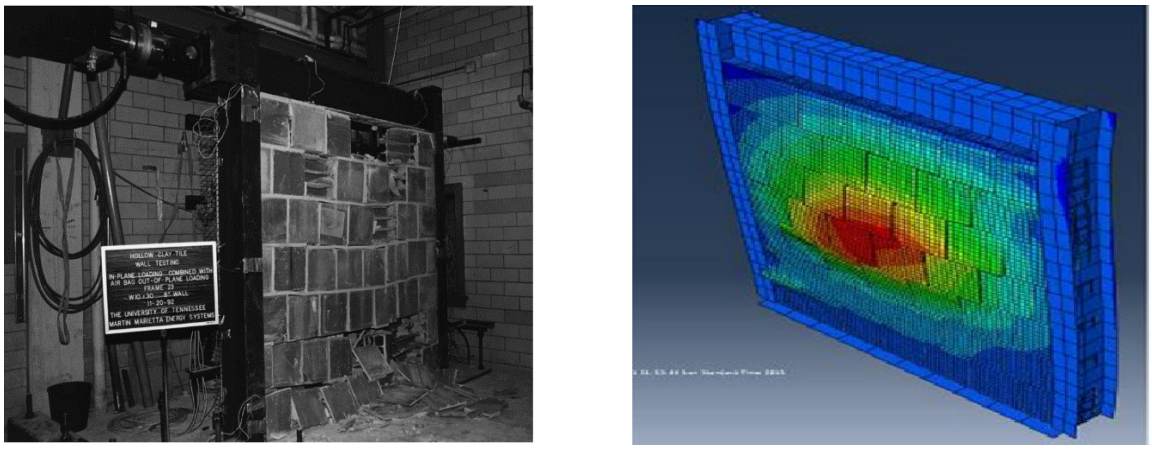

(a) **(b)**

Fig. 5. Comparison and verification of the simulation: (a) Flanagan and Bennett frame[34], (b) finite element model.

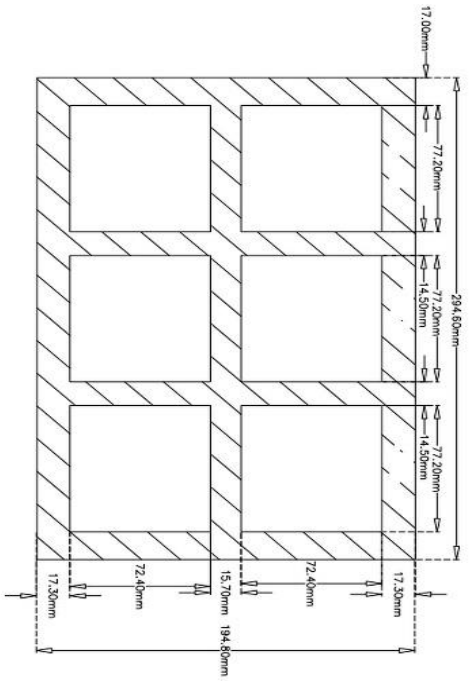

Fig. 6. The geometry of masonry Bricks Unit [35].

Table 6. Characteristics of the considered materials [35, 36]

Tile compressive strength (f'_{cb})	14.8 *MPa*
Compressive strength of coherent masonry material (f'_p)	5.6 *MPa*
Modulus of elasticity of masonry material at x direction (E_x)	5390 *MPa*
Modulus of elasticity of masonry material at y direction (E_y)	2160 *MPa*
Poisson ratio for masonry material (ν)	0.14
Mortar friction coefficient (μ)	0.5-0.7
Specific weight of masonry material (γ)	817 kg/m^3

Fig.7 shows a comparison between the finite element model results and the experimental test results. The evaluation shows a good agreement between the results of the FEM model and experimental test data. The differences between the numerical model and experimental test are due to assumptions of the numerical model.

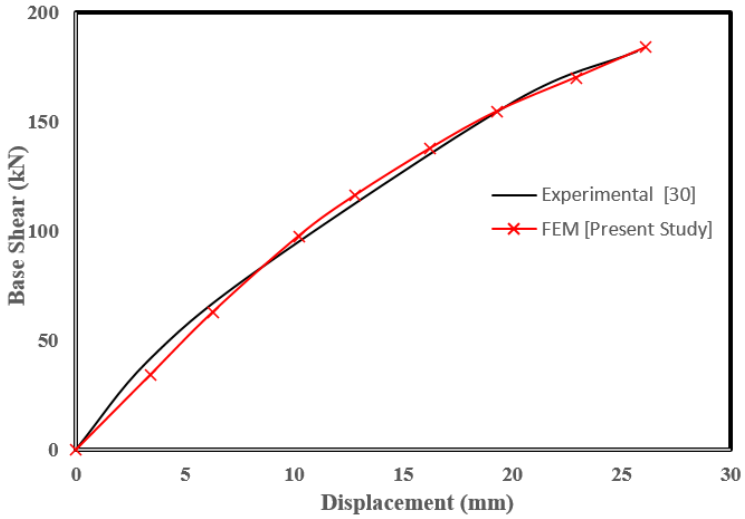

Fig. 7. Comparison between the results of the present study and [35].

4. Results and discussion

In this section, the influence of three parameters such as mechanical properties of polymeric materials (E, u), thickness of isolator layer (t), frame's dimensions (H / B), in reducing the initial stiffness and ultimate strength of masonry infill were investigated. For this purpose, all hysteresis diagrams have been given in Appendix A. Fig. 8-19 were obtained using the diagrams in Appendix A.

Fig. 8 shows the influence of isolator thickness in separating the masonry infill with H/B=0.5. Less stiffness has been observed in the masonry infill frame at a separation thickness of 5 mm in polystyrene and polyurethane materials. In other words, in polystyrene and polyurethane materials, the optimal separation performance in reducing initial stiffness occurs at lower thicknesses. However, in polyethylene and rubber materials, good performance in reducing the initial stiffness occurs at a thickness of 20 mm. Fig. 9 shows the influence of isolator materials in frame with H/B=0.5. The results generally show better performance of polystyrene at small separation thicknesses in reducing the initial stiffness of the masonry infill frame. By increasing the thickness of the isolator, almost all materials showed the same performance in reducing initial stiffness. Also, as the thickness of the isolator increases, the polymeric materials that have a higher elasticity modulus have a better performance. Generally, in isolation infill walls from the surrounding frame with a height to length ratio (H/B=0.5), polymeric materials with lower elasticity modules in lower thickness of isolation have a better performance in reducing initial stiffness. Polymeric materials in masonry infill wall

with H/B=0.5 can reduce the initial stiffness from about 30% (polyurethane in 5 mm thickness) to about 60% (polyethylene in 5mm thickness).

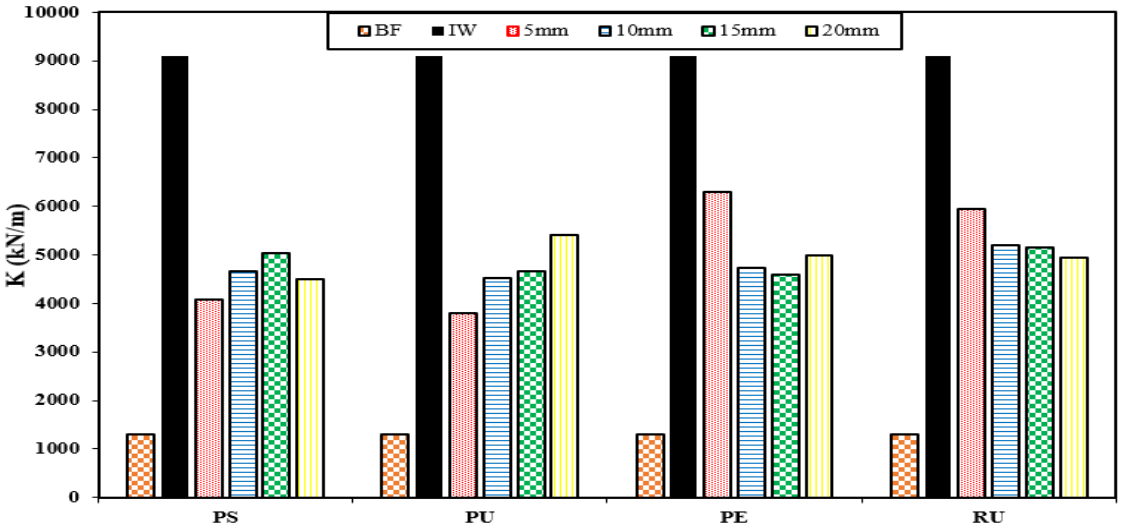

Fig. 8. The influence of isolator layer thickness on reducing the initial stiffness of the masonry infill in frame with H/B=0.5.

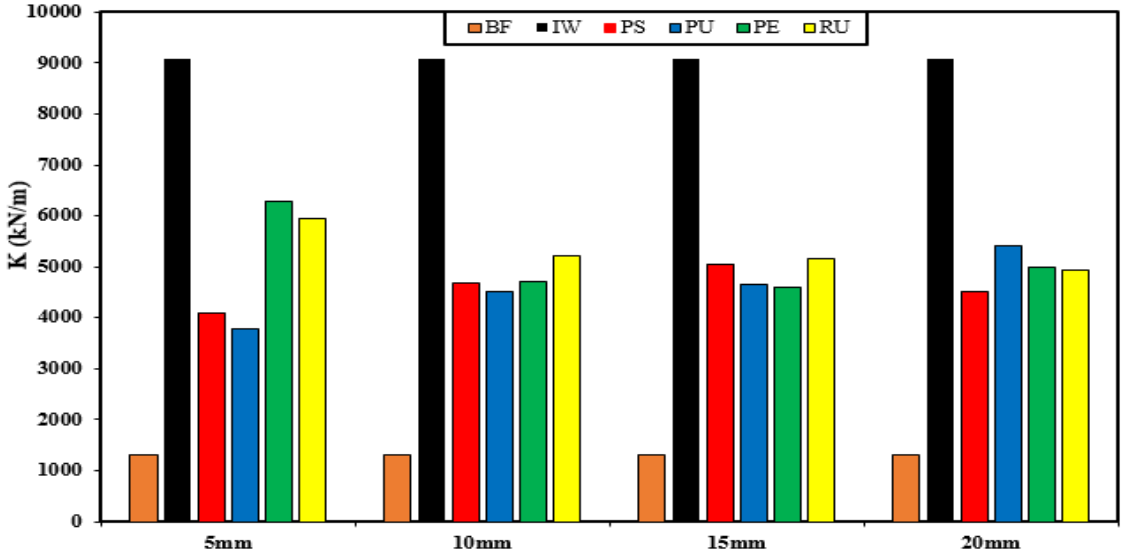

Fig. 9. The influence of isolator layer materials on reducing the initial stiffness of the masonry infill in frame with H/B=0.5.

In isolating the infill wall from the structural frame with H/B=1.0 by polystyrene, polyethylene, and rubber, best performance occurs at a thickness of 10 mm as shown in Fig. 10. Also, the best polyurethane separation thickness is 20 mm and then 10 mm. It can be concluded that the separation of the masonry infill frame with (H/B=1.0) in a thickness of 10 mm indicates its optimal performance in reducing the initial stiffness. As shown in Fig. 11 in the masonry infill with H/B=1.0, the difference in material

performance at thicknesses greater than 5 mm is negligible. But at a thickness of 5 mm, rubber, has more effect in reducing the initial stiffness of the masonry infill frame. The best separation performance in masonry infill frames (H/B = 1.0) occurs in rubber separation with a thickness of 10 mm. The weakest separation performance occurs in masonry infill frames separated by 20 mm polystyrene.

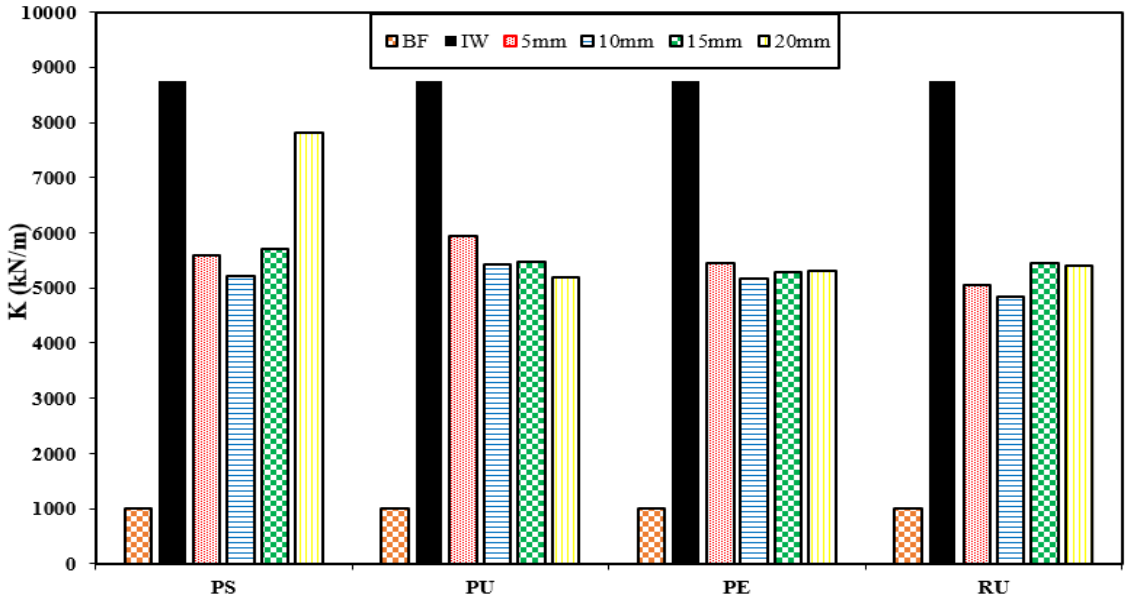

Fig. 10. The influence of isolator layer thickness on reducing the initial stiffness of the masonry infill in frame with H/B=1.0.

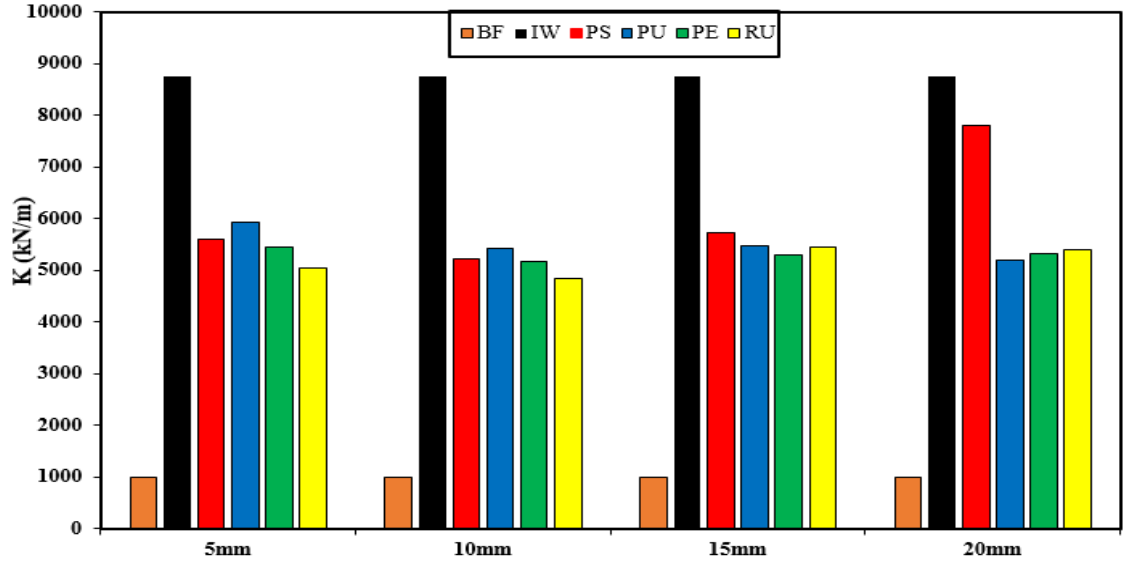

Fig. 11. The influence of isolator layer materials on reducing the initial stiffness of the masonry infill in frame with H/B=1.0.

According to Fig 12, it can be concluded that by increasing the thickness of the isolator up to 15 mm, the isolator performance improves in reducing the initial stiffness, and then in

the separation thickness of 20 mm, the initial stiffness of the masonry infill frame increases. Also, according to Fig. 13, polymeric materials do not significantly reduce stiffness in small isolation thicknesses. Increasing the thickness of the isolator layer in softer polymeric materials such as polystyrene has a more effect in reducing initial stiffness (in H/B=2.0). Generally, the masonry infill frames with (H/B= 2.0) separated by materials with low elasticity modulus have better performance in smaller thicknesses. Separation by materials with a higher modulus of elasticity is also optimal at greater thicknesses.

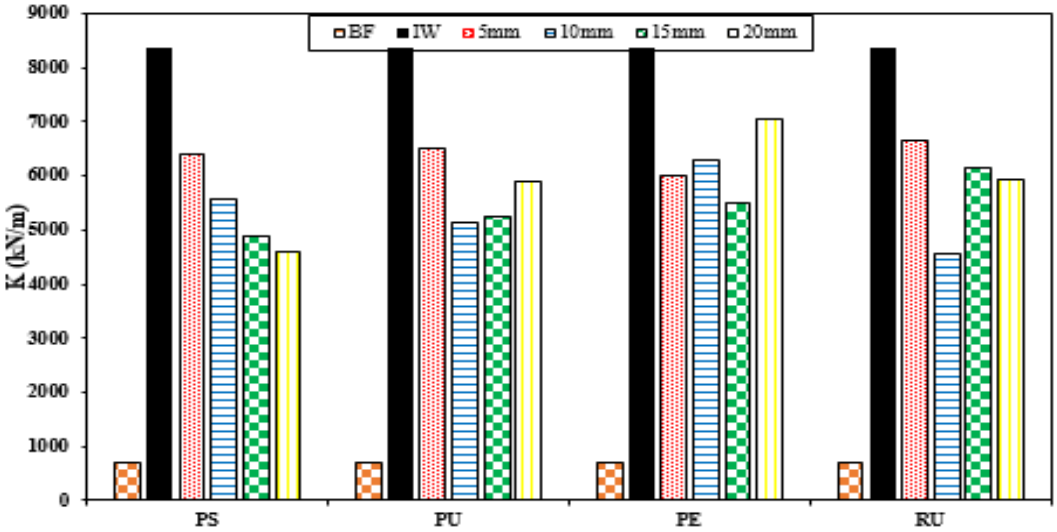

Fig. 12. The influence of isolator layer thickness on reducing the initial stiffness of the masonry infill in frame with H/B=2.0.

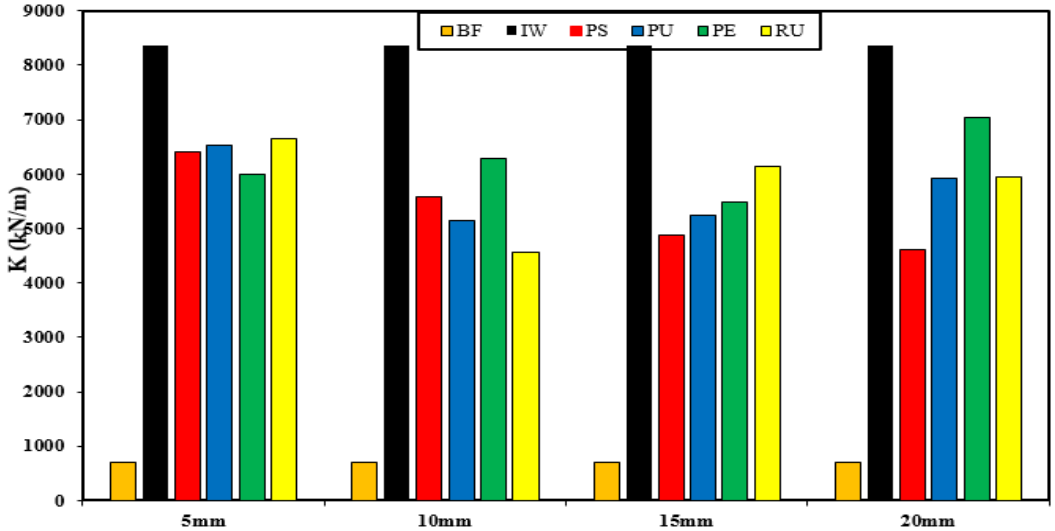

Fig. 13. The influence of isolator layer materials on reducing the initial stiffness of the masonry infill in frame with H/B=2.0.

According to Fig. 14 in a Masonry infill wall with (H / B = 0.5), it can be concluded that in separation with all materials except polystyrene, with increasing separation

thickness, the ultimate strength of the masonry infill frame increases. Also, according to Fig. 15, generally, with increasing the modulus of elasticity of polymeric materials, the ultimate strength of the masonry infill frame increases.

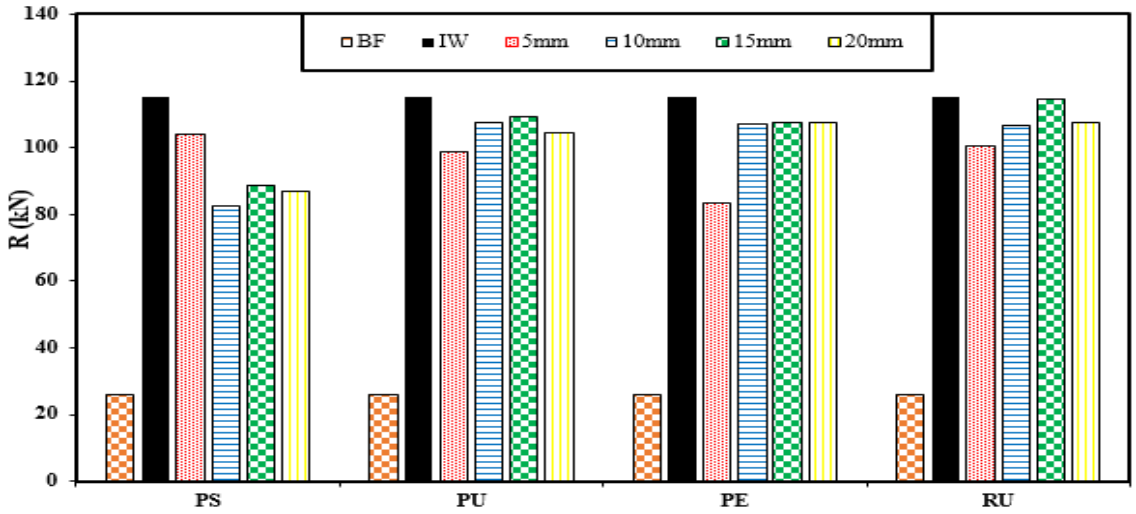

Fig. 14. The influence of isolator layer thickness on reducing the maximum strength of the masonry infill in frame with H/B=0.5.

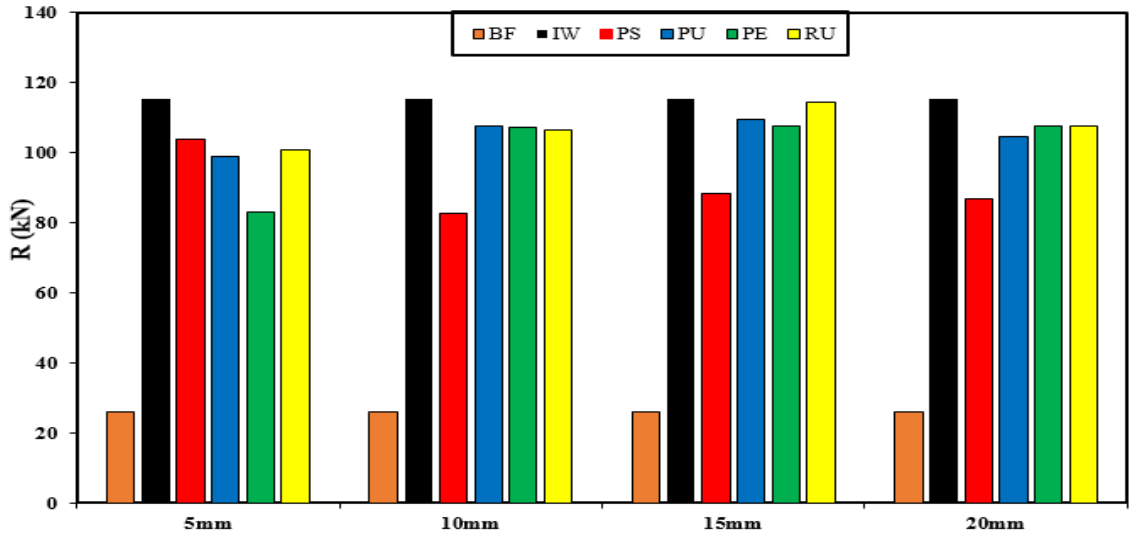

Fig. 15. The influence of isolator layer materials on reducing the maximum strength of the masonry infill in frame with H/B=0.5.

As shown in Fig. 16, in almost all polymeric materials, if the separation is done with a thickness of 5 mm, the ultimate strength of the isolated masonry infill wall does not decrease much. Fig. 17 shows the almost same performance of polymeric materials in isolation thicknesses of 15 and 20 mm. Also, the Masonry infill wall with (H/B=1.0), the polymeric materials do not affect the ultimate strength of the infill wall.

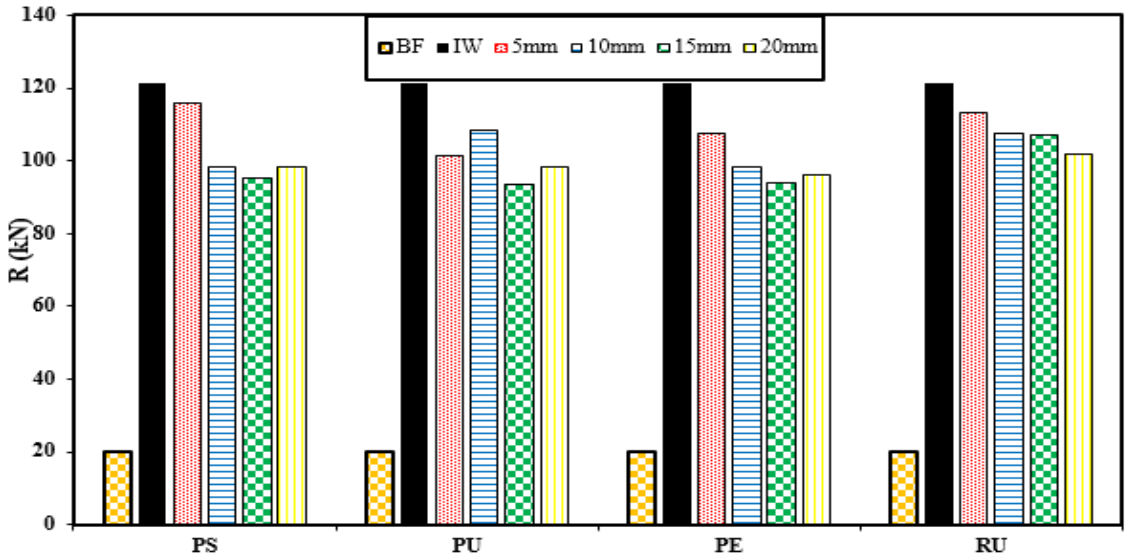

Fig. 16. The influence of isolator layer thickness on reducing the maximum strength of the masonry infill in frame with H/B=1.0.

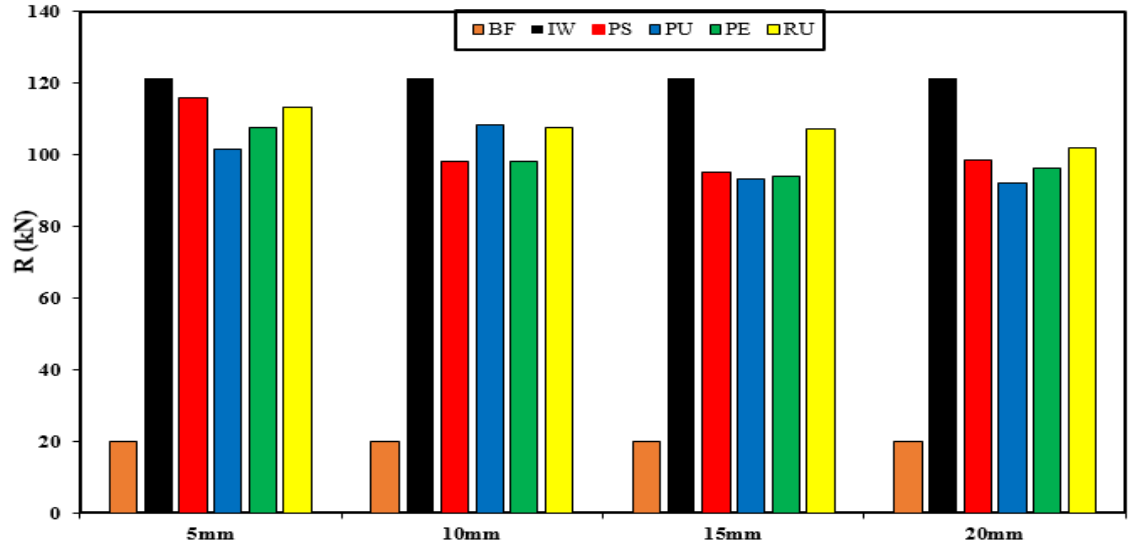

Fig. 17. The influence of isolator layer materials on reducing the maximum strength of the masonry infill in frame with H/B=1.0.

As shown in Fig. 18 and Fig. 19, it can be concluded that the ultimate strength of the isolated infill wall is close to the non-isolated masonry infill wall. However, generally with increasing the thickness of the polymeric materials and increasing the polymeric materials' elastic modulus, the ultimate strength of the isolated masonry wall increases.

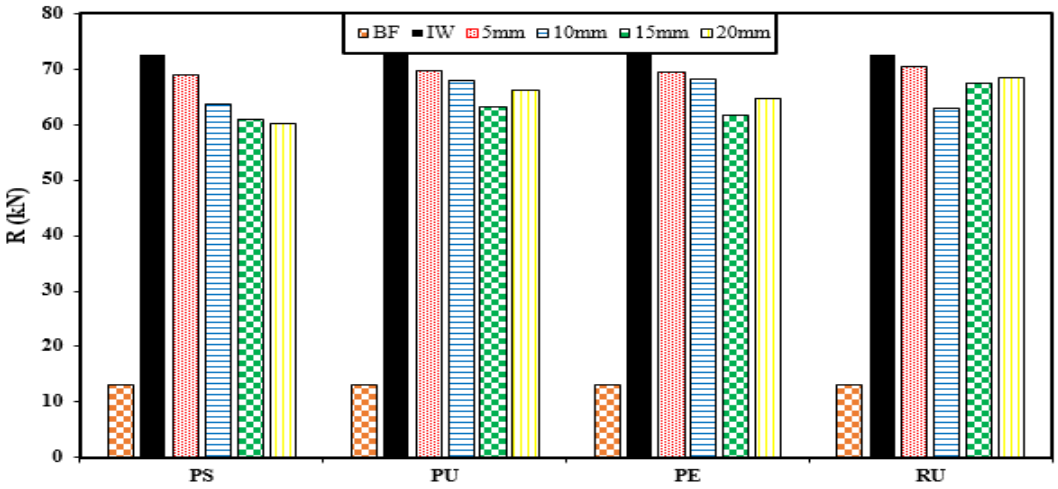

Fig. 18. The influence of isolator layer thickness on reducing the maximum strength of the masonry infill in frame with H/B=2.0.

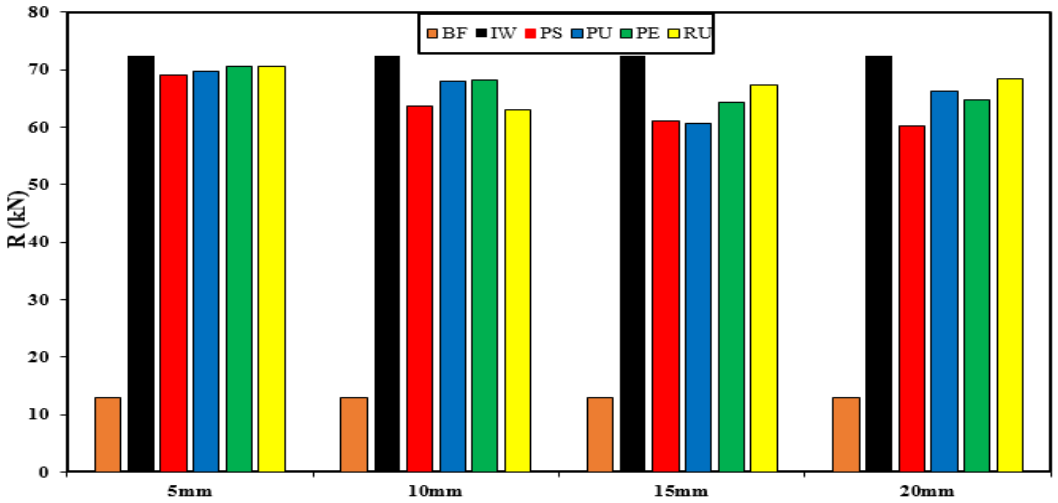

Fig. 19. The influence of isolator layer materials on reducing the maximum strength of the masonry infill in frame with H/B=2.0.

The influence of the ratio of height/length on capacity appears to be small; narrow panels (high ratio of H/B) have substantially higher ductility [40]. The following results were obtained by examining the effect of height-to-length ratio (H/B) of infill wall:

1. Assuming a constant height for the masonry infill wall and increasing the length of the frames lead to an increase in the initial stiffness and the ultimate strength of the masonry infill.

2. In frames with smaller H/B, the separation of masonry infill is more appropriate.

In this section, behavior of masonry infill and isolated masonry infill by 10 mm polyethylene are discussed and compared.

According to Fig. 20a, in constant drift (2%), the isolated infill undergoes less base reaction. In a 2% drift, the isolated masonry infill can reduce the base reaction by up to 25%.

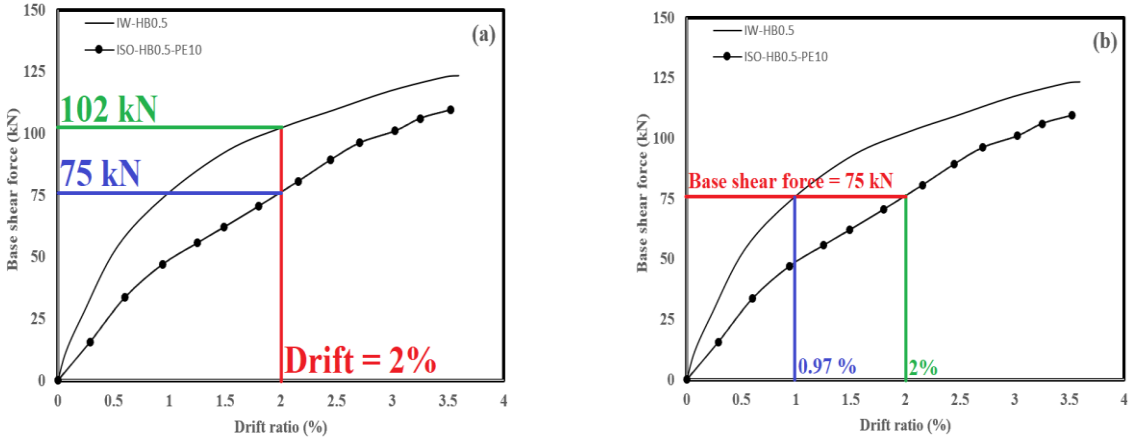

Fig 20. Comparison between the behavior of masonry infill (IW-HB0.5) and masonry isolated infill (ISO-HB0.5-PE10): (a) in constant drift; (b) in constant Base shear force.

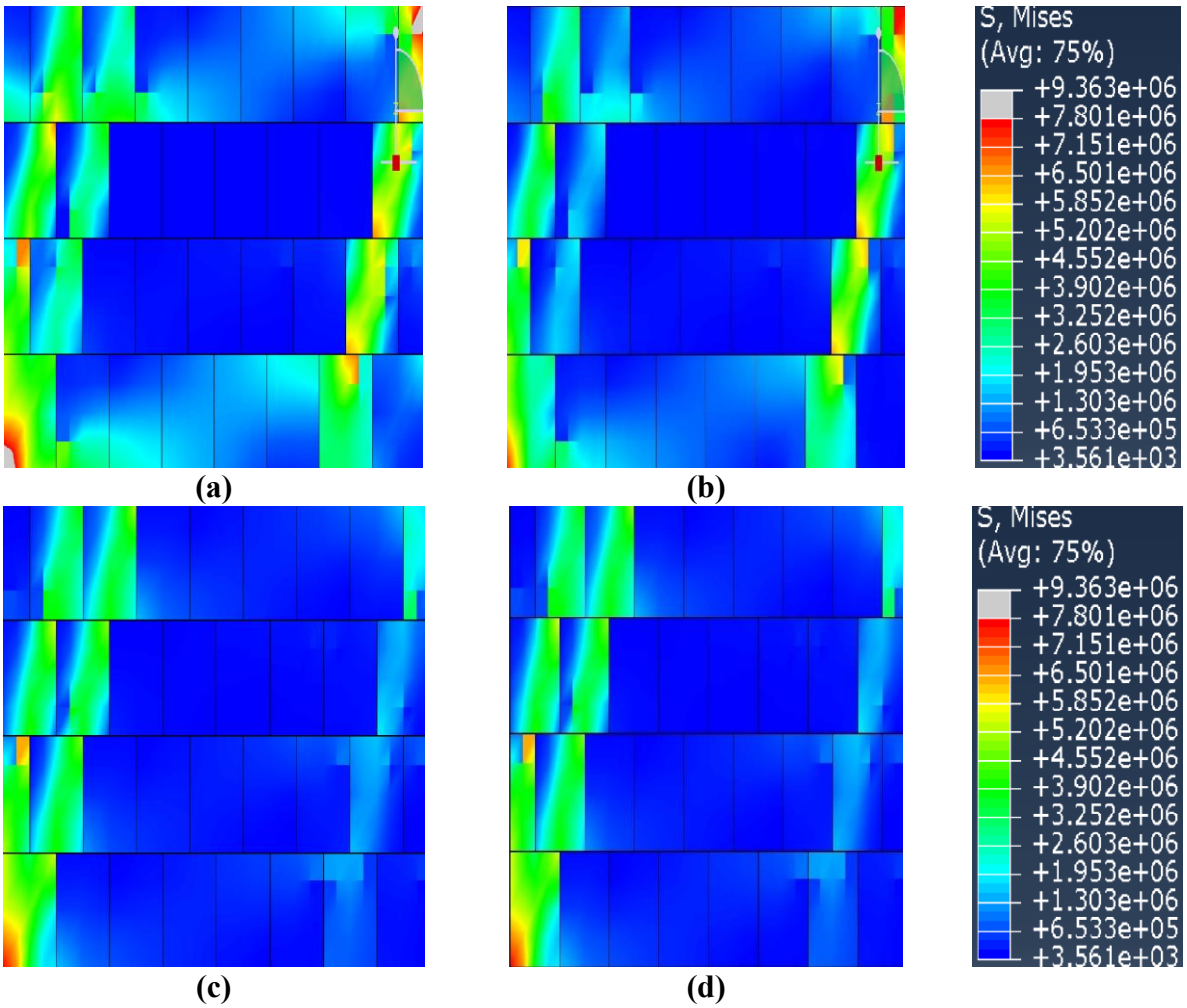

Fig 21. Stress Contour of Masonry Bricks, (a) IW-HB0.5 in Drift= 2%; (b) IW-HB0.5 in Base shear force=75 kN; c) ISO-HB0.5-PE10 in Drift =2%; (d) ISO-HB0.5-PE10 in Reaction Force=75 kN.

Table 7. Effect of separation on initial stiffness and ultimate strength.

H/B	K-IW (kN/m)	R-IW (kN/m)	Material	Thickness(mm)	K(kN/m)	%[1]	R(kN)	%[1]
0.5	9093.95	115.37	PU	5	3787	58	98.75	14
				10	4512	50	107.70	6
				15	4655	48	109.45	5
				20	5404	40	104.46	9
			PS	5	4081	55	103.89	10
				10	4669	48	82.53	28
				15	5046	44	88.53	23
				20	4505	50	86.73	24
			PE	5	6292	30	83.21	27
				10	4723	48	107.08	7
				15	4599	49	107.74	7
				20	4989	45	107.54	6
			RU	5	5945	34	100.67	12
				10	5209	42	106.53	7
				15	5162	43	114.5	1
				20	4940	45	107.54	7
1.0	8753	121.53	PU	5	5940	32	101.38	16
				10	5431	37	108.32	10
				15	5484	37	93.42	23
				20	5188	40	92.15	24
			PS	5	5589	36	115.96	4
				10	5209	40	98.19	19
				15	5717	34	95.31	21
				20	7806	10	98.55	18
			PE	5	5442	37	107.62	11
				10	5166	40	98.33	19
				15	5295	39	93.88	22
				20	5311	39	96.32	20
			RU	5	5042	42	113.42	6
				10	4833	44	107.59	11
				15	5459	37	107.16	11
				20	5403	38	101.90	16
2.0	8360	72.47	PU	5	6519	22	69.72	4
				10	5137	38	67.86	6
				15	5244	37	60.66	16
				20	5913	29	66.18	8
			PS	5	6416	23	69	4
				10	5573	53	63.63	12
				15	4890	44	61.03	15
				20	4603	44	60.15	16
			PE	5	5997	28	70.45	2
				10	6297	24	68.16	5
				15	5485	34	64.34	11
				20	7044	15	64.67	10
			RU	5	6646	20	70.5	2
				10	4573	45	67.97	13
				15	6143	26	67.36	7
				20	5941	28	68.5	5

[1] Reduction rate of initial stiffness and ultimate strength

Also, in a constant base reaction (75 kN), the drift amount increased about two times compared with the masonry infill's unseparated infill wall. It means that the ductility increases with the separation of the infill wall (Fig. 20b). By comparing the stress contour in a constant drift (2%), it can be derived that the isolation of masonry infill by polymeric materials can reduce the stress of clay blocks (Fig. 21a, Fig. 21c). According to Figure (Fig. 21b, Fig. 21d), the separation of the masonry infill in a constant base reaction (75 kN) can decrease the masonry bricks' stress. In order to have clearly conclusions, in Table 7, the percentage of reduction in initial stiffness and ultimate strength is shown.

5. Conclusions

This article investigated a procedure for separating masonry infills from structural frames during deformation. The high deformation capacity behavior of polymeric materials is vital for isolating infill walls from the frame. According to the proposed concept, isolating masonry infill from the frame using polymeric material has an excellent potential to reduce infill wall-frame interactions. Therefore, the behavior of infilled frames is similar to bare frames.

Frame dimensions, the isolator layer's thickness, and the isolator materials were investigated. In general, the separation of masonry infill in frames with a lower height-to-length (H/B) ratio shows better performance of isolation effect. In isolation infill walls from the surrounding frame with H/B=0.5, polymeric materials with lower elasticity modules in lower thickness of isolation have a better performance in reducing initial stiffness. In this case, polymeric layers can reduce the initial stiffness from about 30% (polyurethane in 5 mm thickness) to about 60% (polyethylene in 5mm thickness). The best separation performance in masonry infill frames (H/B = 1.0) occurs in rubber separation with a thickness of 10 mm. Also, polymeric materials do not significantly reduce stiffness in small isolation thicknesses. Increasing the isolator layer's thickness in softer polymeric materials such as polystyrene has more potential in reducing initial stiffness (in H/B=2.0). In all height to length ratios of the frame, separation by polymeric materials with a higher modulus of elasticity is also optimal at greater thicknesses. As well as, using softer isolator materials with less thickness leads to a more appropriate masonry infill behavior. In addition, in constant drift, the isolated infill experiences a lower base reaction of up to 25%. Also, in constant base reaction, the drift amount increases to 100% with the masonry infill's separation. It means that the ductility increases with the separation of the infill wall.

Overall, isolating the masonry wall from the structural frame using polymeric material is an excellent idea to decrease the damage to the structure and masonry infill.

Futures studies can be considered more materials for isolating. Also, geometric isolator optimization can be a good idea to continue research. In addition, due to the effects of opening on masonry infill wall behavior mentioned in [41]. In future research, the separation of openings from masonry walls by polymeric materials can be investigated.

Appendix

Hysteresis diagrams of base-shear vs. displacement are represented in this part for models with different properties.

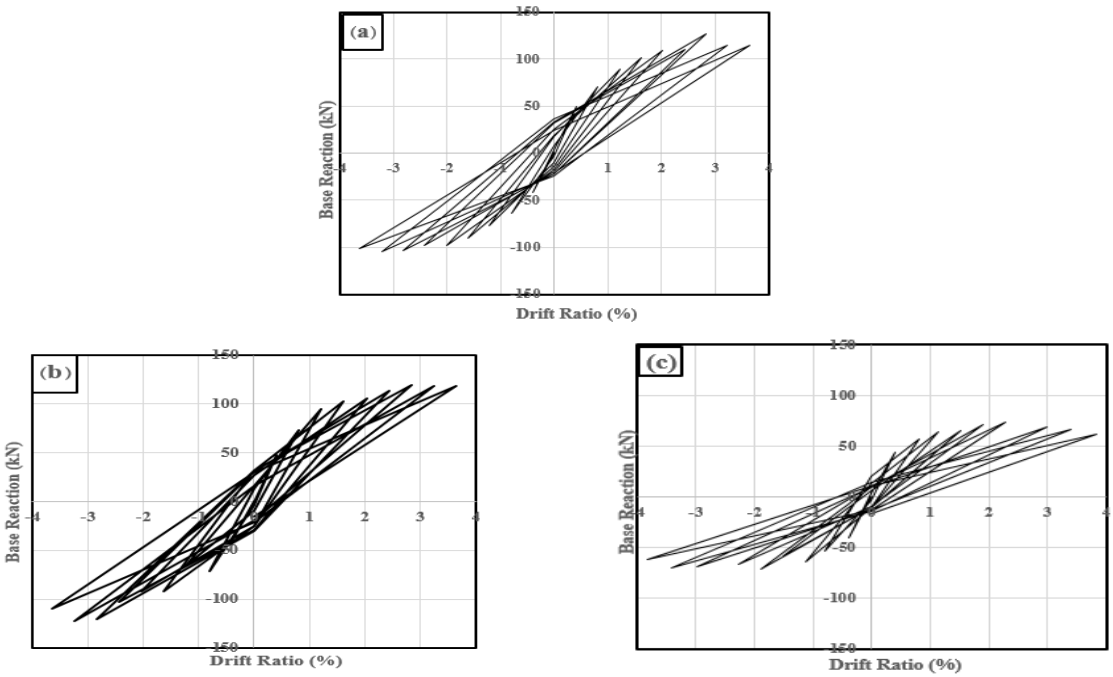

Fig A. 1. Hysteretic loop of Bare frame: (a) BF-HB0.5, (b) BF-HB1.0, (c) BF-HB2.0.

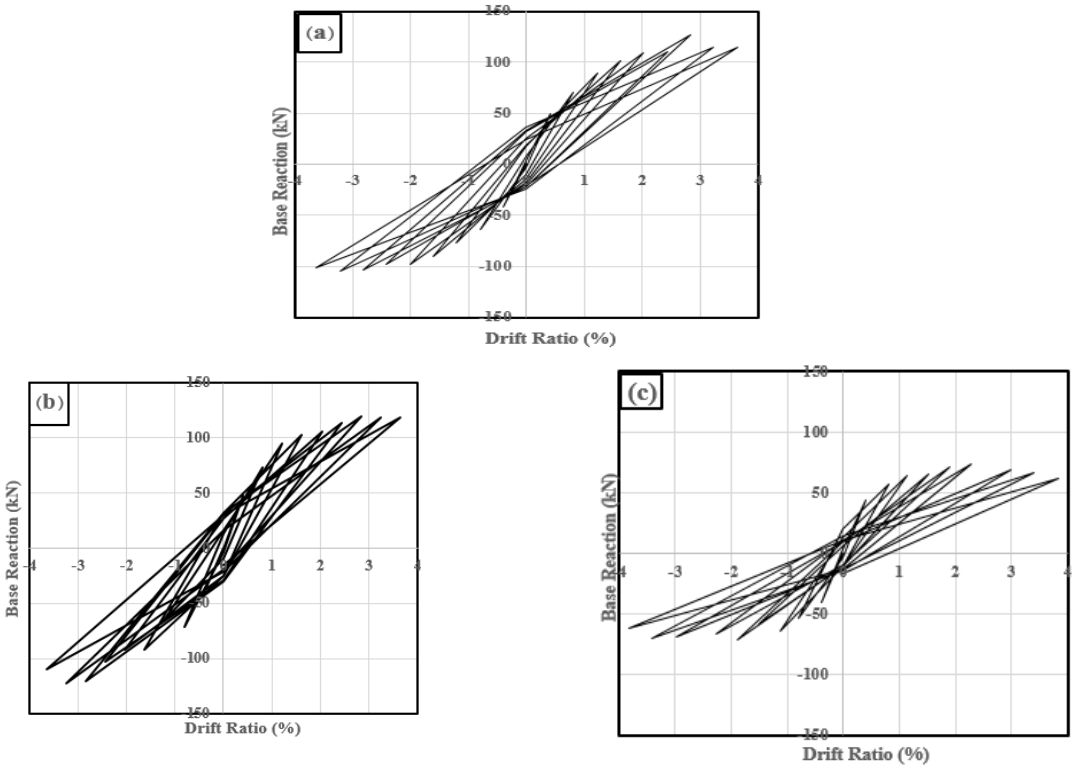

Fig A. 2. Hysteretic loop of Infill Wall: (a) IW-HB0.5, (b) IW-HB1.0, (c) IW-HB2.0.

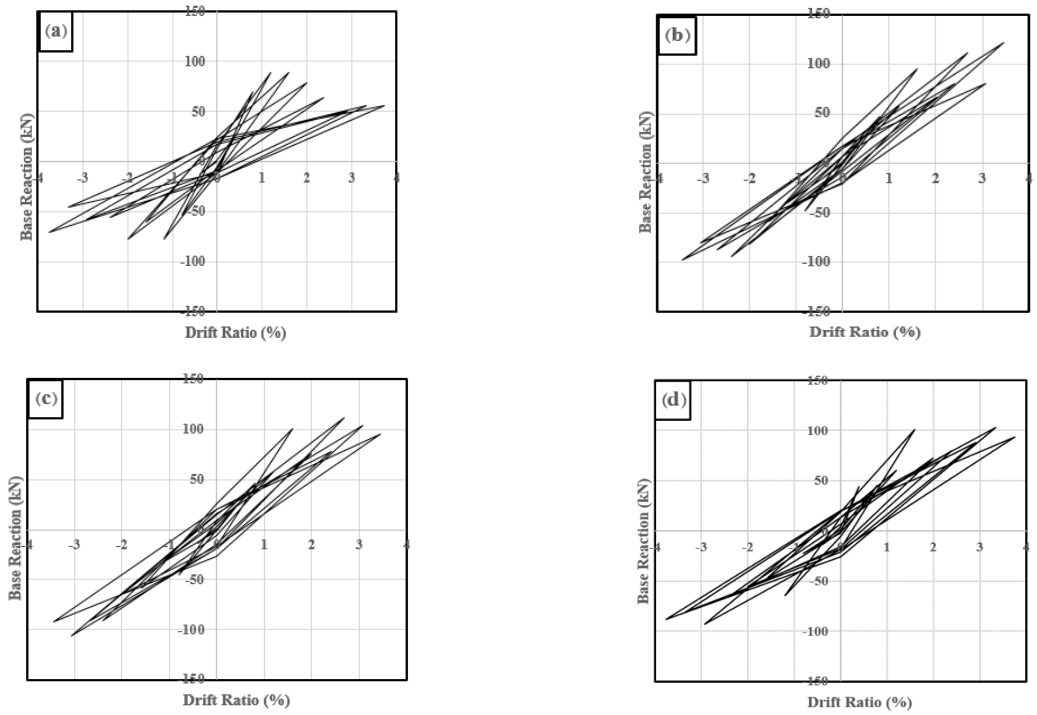

Fig A. 3. Hysteretic loop of Isolated infill: (a) ISO-HB0.5-PU5, (b) ISO-HB0.5-PU10, (c) ISO-HB0.5-PU15, ISO-HB0.5-PU20.

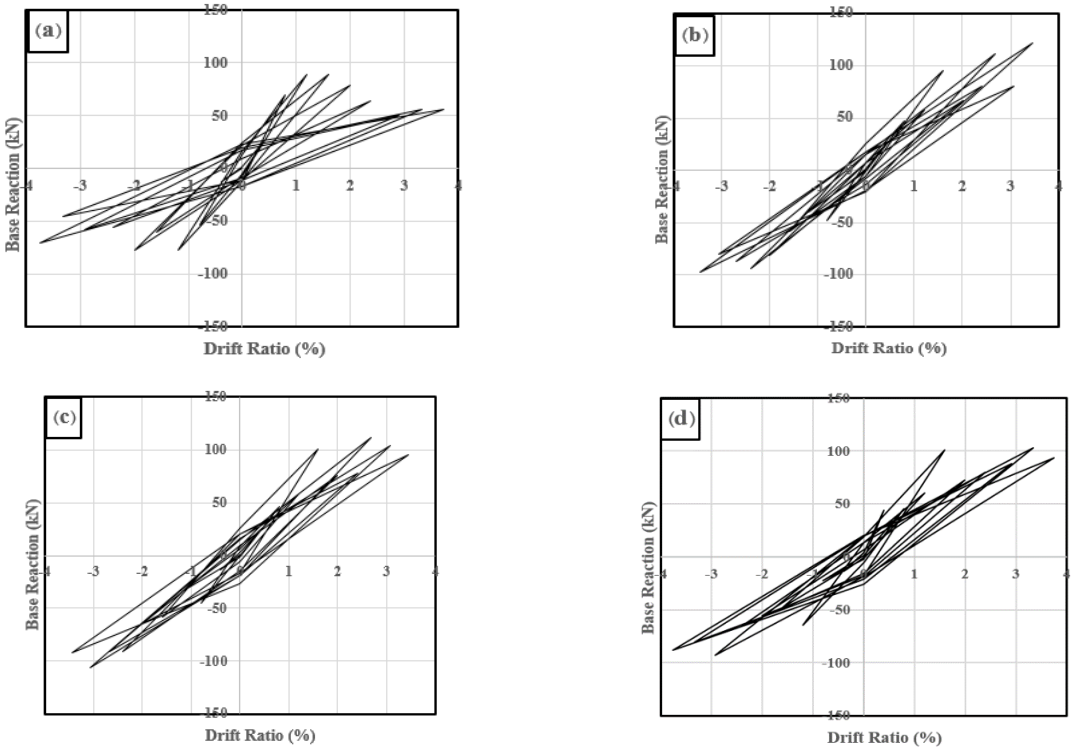

Fig A. 4. Hysteretic loop of Isolated infill: (a) ISO-HB0.5-PS5, (b) ISO-HB0.5-PS10, (c) ISO-HB0.5-PS15, ISO-HB0.5-PS20.

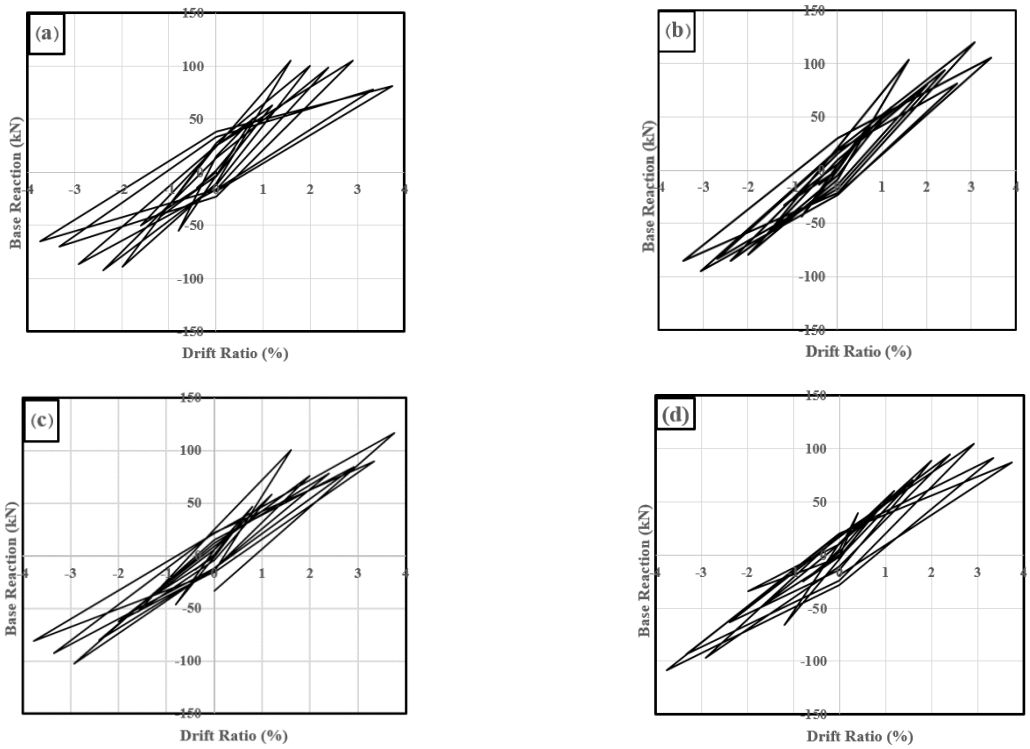

Fig A. 5. Hysteretic loop of Isolated infill: (a) ISO-HB0.5-PE5, (b) ISO-HB0.5-PE10, (c) ISO-HB0.5-PE15, ISO-HB0.5-PE20.

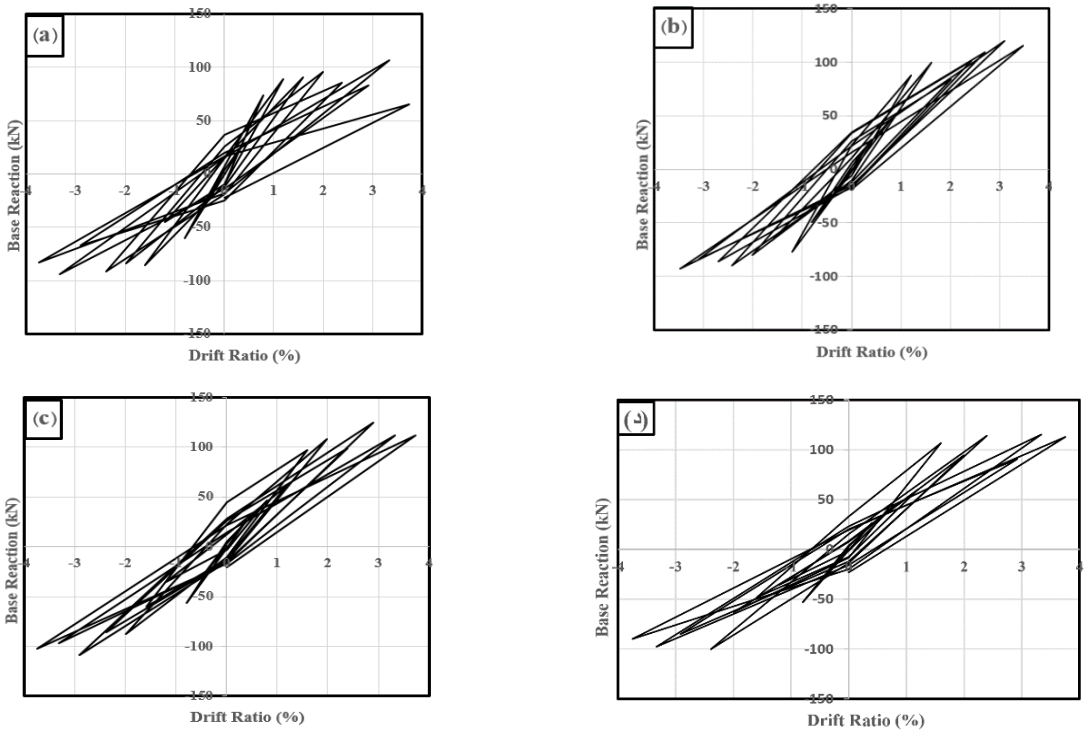

Fig A. 6. Hysteretic loop of Isolated infill: (a) ISO-HB0.5-RU5, (b) ISO-HB0.5-PR10, (c) ISO-HB0.5-RU15, ISO-HB0.5-RU20.

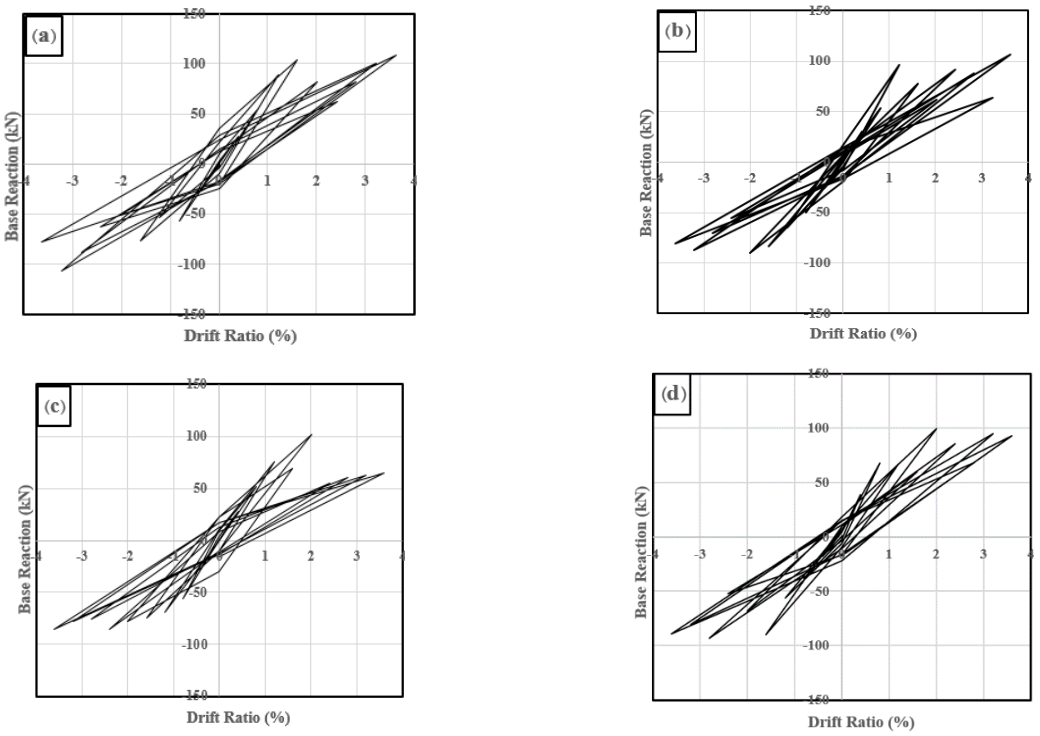

Fig A. 7. Hysteretic loop of Isolated infill: (a) ISO-HB1.0-PU5, (b) ISO-HB1.0-PU10, (c) ISO-HB1.0-PU15, ISO-HB1.0-PU20.

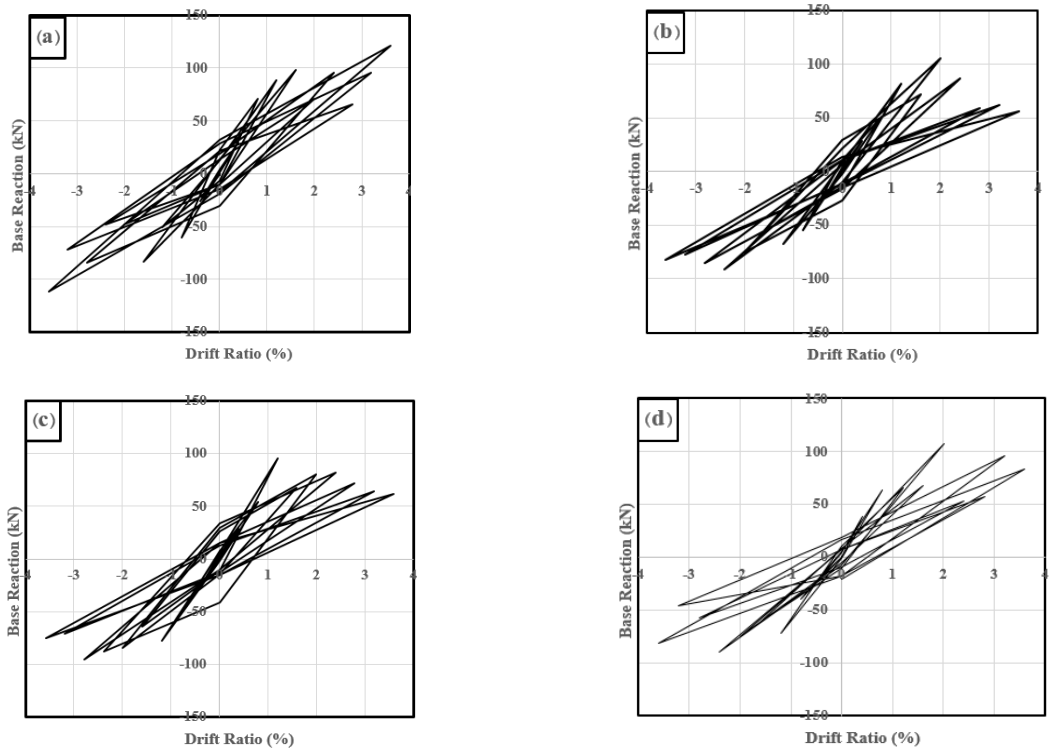

Fig A. 8. Hysteretic loop of Isolated infill: (a) ISO-HB1.0-PS5, (b) ISO-HB1.0-PS10, (c) ISO-HB1.0-PS15, ISO-HB1.0-PS20.

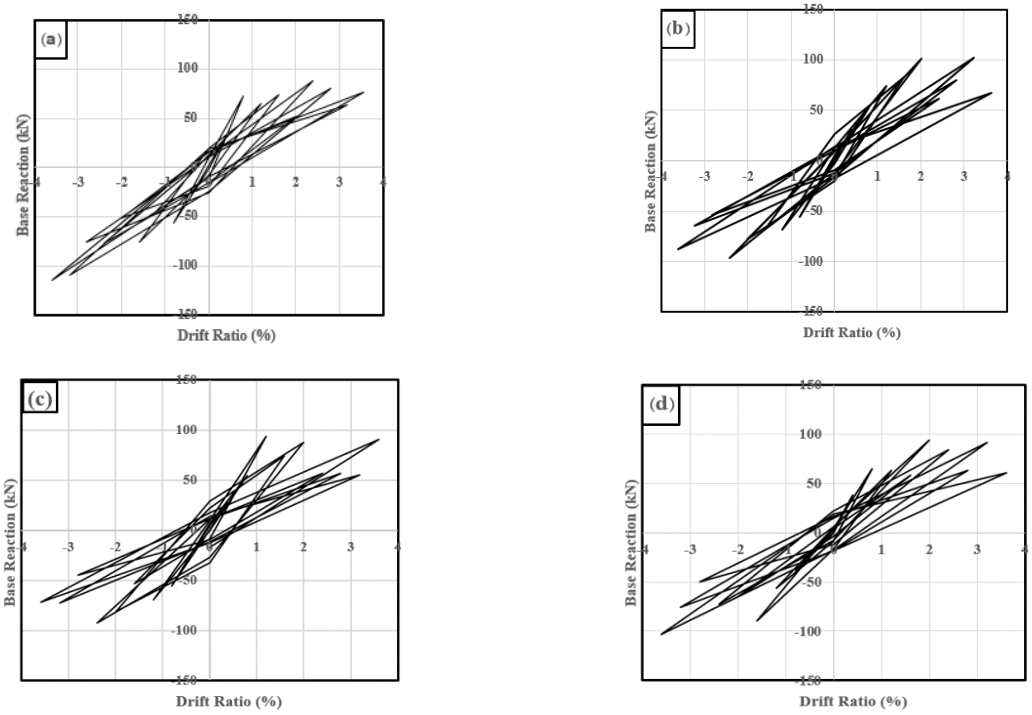

Fig A. 9. Hysteretic loop of Isolated infill: (a) ISO-HB1.0-PE5, (b) ISO-HB1.0-PE10, (c) ISO-HB1.0-PE15, ISO-HB1.0-PE20.

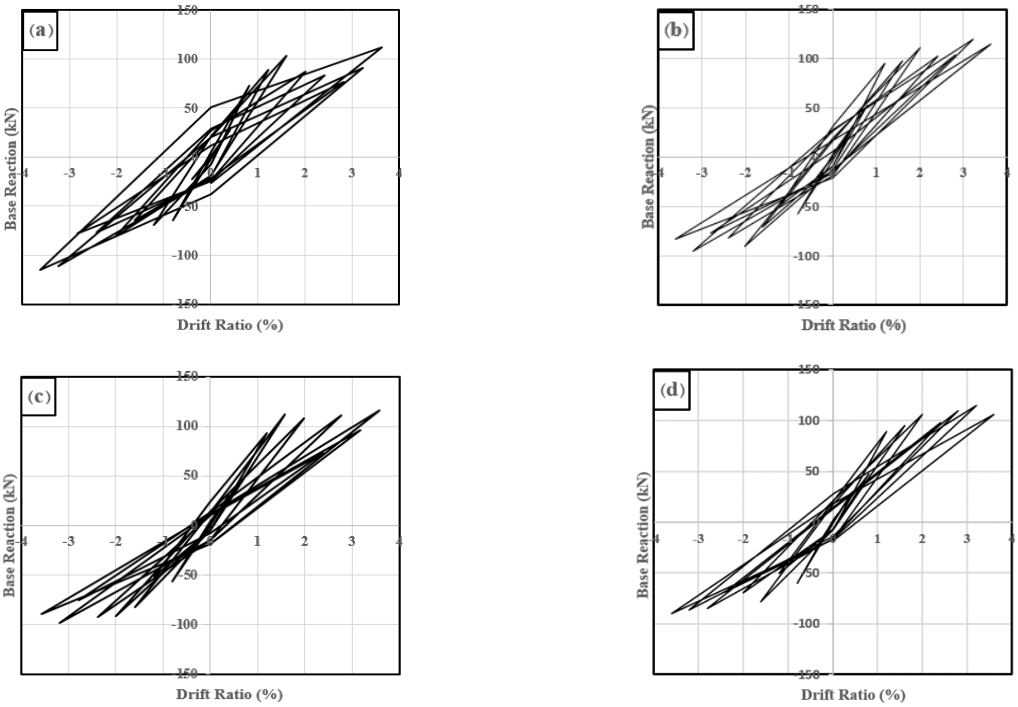

Fig A. 10. Hysteretic loop of Isolated infill: (a) ISO-HB1.0-RU5, (b) ISO-HB1.0-RU10, (c) ISO-HB1.0-RU15, ISO-HB1.0-RU20.

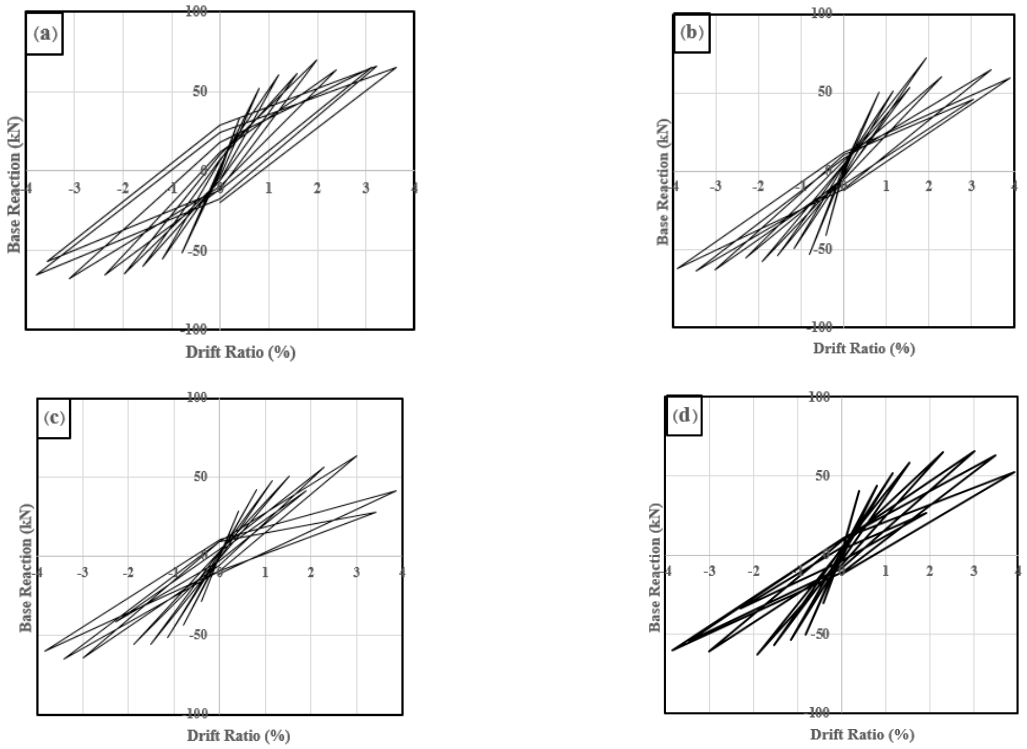

Fig A. 11. Hysteretic loop of Isolated infill: (a) ISO-HB2.0-PU5, (b) ISO-HB2.0-PU10, (c) ISO-HB2.0-PU15, ISO-HB2.0-PU20.

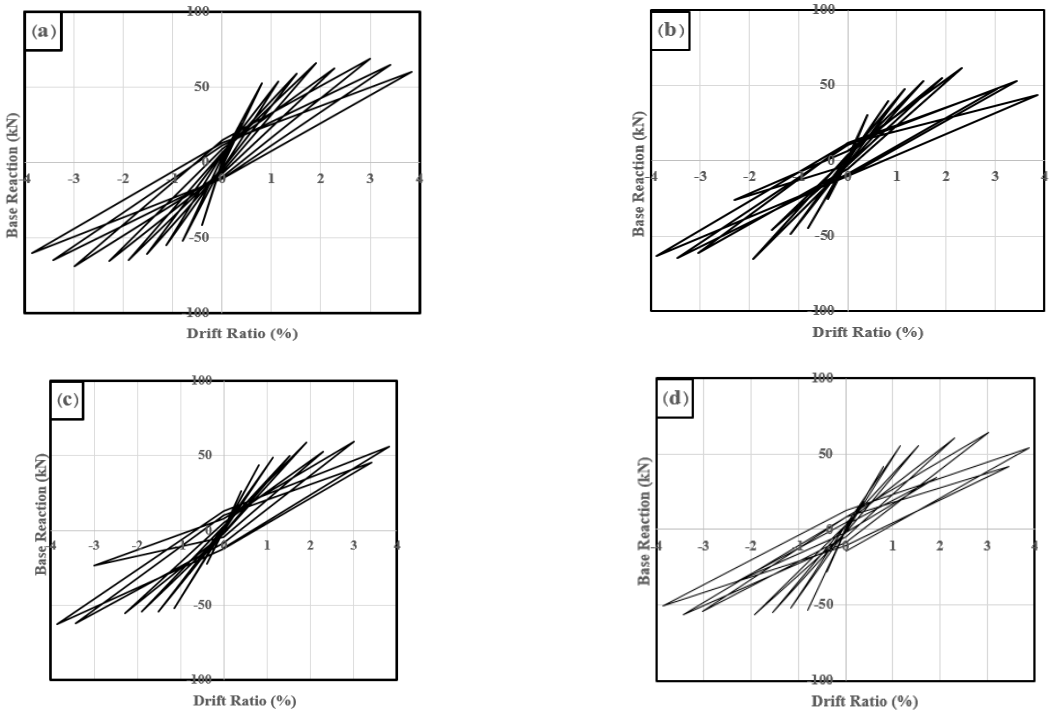

Fig A. 12. Hysteretic loop of Isolated infill: (a) ISO-HB2.0-PS5, (b) ISO-HB2.0-PS10, (c) ISO-HB2.0-PS15, ISO-HB2.0-PS20.

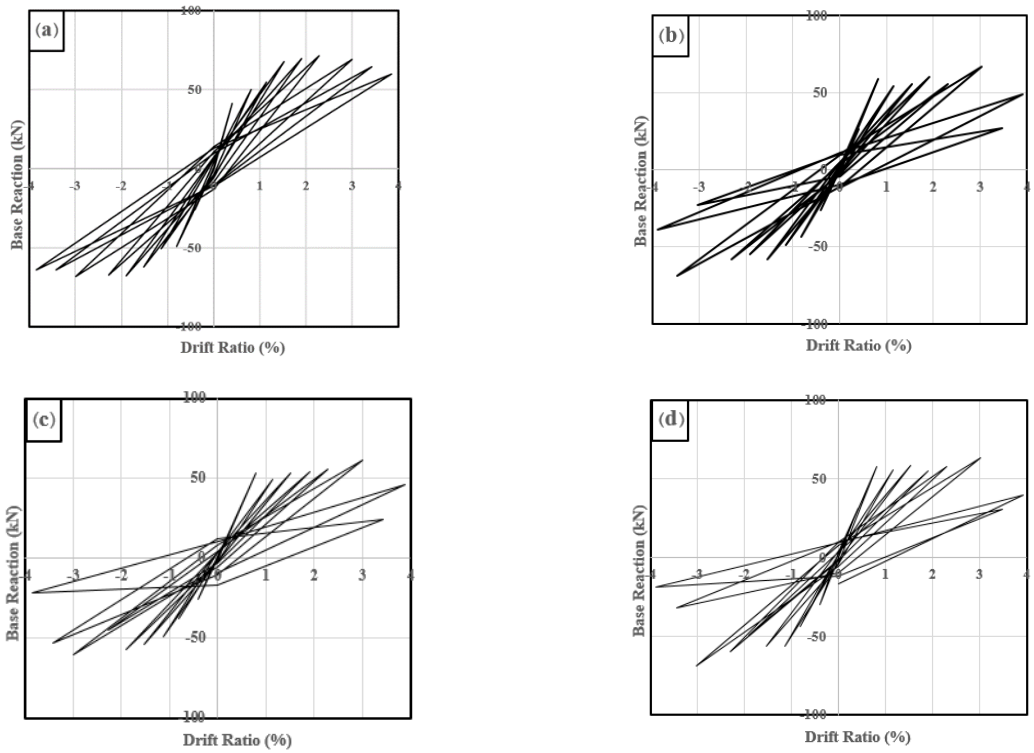

Fig A. 13. Hysteretic loop of Isolated infill: (a) ISO-HB2.0-PE5, (b) ISO-HB2.0-PE10, (c) ISO-HB2.0-PE15, ISO-HB2.0-PE20.

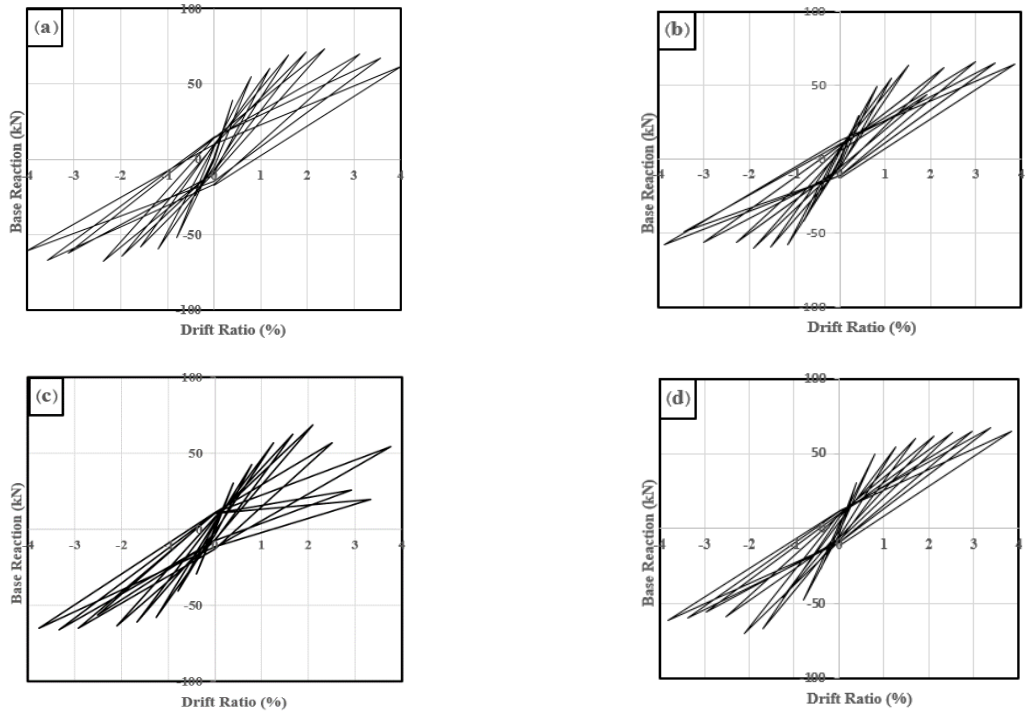

Fig A. 14. Hysteretic loop of Isolated infill: (a) ISO-HB2.0-RU5, (b) ISO-HB2.0-RU10, (c) ISO-HB2.0-RU15, ISO-HB2.0-RU20.

References

[1] Fardis, M.N., Panagiotakos, T.B. (1997). "Seismic design and response of bare and infilled reinforced concrete buildings – part ii: infilled structures." Journal of Earthquake Engineering, Vol. 01, pp. 475-503. doi:10.1080/13632469708962375

[2] Negro, P., Colombo, A. (1997). "Irregularities induced by nonstructural masonry panels in framed buildings." Engineering Structures. Vol. 19, Issue 7, pp. 576–585. doi:10.1016/S0141-0296(96)00115-0

[3] Centeno, J., Ventura, C., Foo, S., Lara, O. (2008). "Seismic performance of gravity load designed reinforced concrete frames with unreinforced masonry infill walls." In: Structures Congress. pp. 1–13. doi:10.1061/41016(314)115

[4] Jalaeefar, A., Zargar, A. (2020). "Effect of infill walls on behavior of reinforced concrete special moment frames under seismic sequences." In Structures. Vol. 28, pp. 766–773. doi:10.1016/j.istruc.2020.09.029

[5] Torkian, Z., Khodakarami, M.I. (2022). "Development of Fragility Curves for Brick Infill Walls in Steel Frame Structures." Journal of Rehabilitation in Civil Engineering, Vol. 10, Issue4. doi:10.22075/jrce.2021.21646.1453

[6] Filiatrault, A., Sullivan, T. (2014). "Performance-based seismic design of nonstructural building components: The next frontier of earthquake engineering." Earthquake Engineering and Engineering Vibration. Vol. 13, pp. 17–46. doi:10.1007/s11803-014-0238-9

[7] Villaverde, R. (1997). "Seismic design of secondary structures: state of the art." Journal of structural engineering. Vol. 23, pp. doi:1011–1019. 10.1061/(ASCE)0733-9445(1997)123:8(1011)

[8] Raddington JR. (1984). "The influence of initial gaps on infilled frame behavior." In: Proceedings of Institution of Civil Engineer Part II, pp. 295–310.

[9] Ju, R.S., Lee, H.J., Chen, C.C., Tao, C.C. (2012). "Experimental study on separating reinforced concrete infill walls from steel moment frames." Journal of Constructional Steel Research. Vol. 71, pp. 119–128. doi: 10.1016/j.jcsr.2011.10.004

[10] Kuang, J.S., Wang. Z. (2017). "Cyclic load tests of RC frame with column-isolated masonry infills." In: Proceedings of the 2nd European Conference on Earthquake Engineering and Seismology (2ECEES), Istanbul, Turkey; pp. 25-29.

[11] Chen, X., Liu, Y. (2017). "Finite Element Study of the Effect of Interfacial Gaps on the in-Plane Behaviour of Masonry Infills Bounded by Steel Frames." Structures, Vol. 10**,** pp. 1–12. doi: 10.1016/j.istruc.2016.11.001

[12] Hu, C., Liu, Y. (2015). "Effects of Interfacial Gaps on the In-Plane Behaviour of Masonry Infilled RC Frames." GEN. 44, p1.

[13] Prakash, S.S., Alagusundaramoorthy, P. (2007). "Study on Brick Masonry Infill Walls With Air Gap." In: 9th Canadian Conference on Earthquake Engineering, Ottawa, Ontario, Canada.

[14] Rezaee Manesh, M., Fattahi, S., & Saffari, H. (2020). Investigation of Earthquake Significant Duration on the Seismic Performance of Adjacent Steel Structures in Near-Source. Journal of Rehabilitation in Civil Engineering, 9(1), 84–101. https://doi.org/10.22075/jrce.2020.20373.1410

[15] Gupta VV, Reddy G, Pendhari SS. Response Control of Structures Subjected to Multi-Hazards of Earthquake and Wind Using Base Isolators and Absorbers. Comput Eng Phys Model 2022;5:19–44. https://doi.org/10.22115/CEPM.2022.317125.1192.

[16] Chabokan E, Faridmehr I. Seismic Assessment of Steel Moment Frames with Irregularity in Mass and Stiffness. Comput Eng Phys Model 2018;1:71–89. https://doi.org/10.22115/cepm.2018.141604.1039.

[17] Siddika A, Awall M, Mamun M, Al A, Humyra T. Study on natural frequency of frame structures. Comput Eng Phys Model 2019;2:36–48.

[18] Lin, K., Totoev, Y.Z., Liu, H.J. (2011). "In-plane cyclic test on framed dry-stack masonry panel." In Advanced materials research. Vol. 163, pp. 3899–903. doi:10.4028/www.scientific.net/AMR.163-167.3899.

[19] Mohammadi, M., Akrami, V., Mohammadi-Ghazi, R. (2011). "Methods to Improve Infilled Frame Ductility." Journal of Structural Engineering, Vol. 137, Issue 6, pp. 646–653. doi: 10.1061/(ASCE)ST.1943-541X.0000322

[20] Misir, I.S., Ozcelik, O., Girgin, S.C., Kahraman, S. (2012). "Experimental work on seismic behavior of various types of masonry infilled RC frames." Structural Engineering and Mechanics. Vol. 44, Issue 6, pp. 763–774.

doi: 10.12989/sem.2012.44.6.763

[21] Preti, M., Bettini, N., Plizzari, G. (2012). "Infill walls with sliding joints to limit infill-frame seismic interaction: large-scale experimental test." Journal of Earthquake Engineering, Vol. 16, Issue 1, pp. 125–141. doi:10.1080/13632469.2011.579815

[22] Bolis, V., Stavridis, A., Preti, M. (2017). "Numerical Investigation of the In-Plane Performance of Masonry-Infilled RC Frames with Sliding Subpanels." Journal of Structural Engineering, Vol. 143, Issue 2.

doi: 10.1061/(ASCE)ST.1943-541X.0001651

[23] Preti, M., Bettini, N., Migliorati, L., Bolis, V., Stavridis, A., Plizzari, G.A. (2016). "Analysis of the in-plane response of earthen masonry infill panels partitioned by sliding joints." Earthquake Engineering & Structural Dynamics, Vol. 45, Issue 8, pp. 1209-1232.doi: 10.1002/eqe.2703

[24] Markulak, D., Radic, I., Sigmund, V. (2013). "Cyclic testing of single bay steel frames with various types of masonry infill." Engineering structures, Vol. 51, pp. 267–277. doi: 10.1016/j.engstruct.2013.01.026

[25] Aliaari, M. (2005). "Development of seismic infill wall isolator subframe (SIWIS) system." Ph.D. thesis, Department of

Architectural Engineering, Penn State University, University Park.

[26] Tasligedik, A.S. (2014). "Damage mitigation strategies for non-structural infill walls." Ph.D. thesis, Department of Civil Engineering, University of Canterbury.

[27] Lin, K., Totoev, Y., Liu, H., Guo, T. (2016). "In-Plane Behaviour of a Reinforcement Concrete Frame with a Dry Stack Masonry Panel." Materials, Vol. 9 Issue 2. doi:10.3390/ma9020108

[28] Mohammadi, M., Akrami, V., Mohammadi-Ghazi, R. (2011), "Methods to improve infilled frame ductility." Journal of Structural Engineering, Vol. 137, Issue 6, pp. 646-653.

doi: 10.1061/(ASCE)ST.1943-541X.0000322

[29] Mohammadi Nikoo, M., Akhaveissy, A. H., Permanoon, A. (2021). "An Investigation of Performance of Masonry Wall Reinforced with Timber lumbers." Journal of Rehabilitation in Civil Engineering, Vol.9, Issue 1, pp. 114-138. doi: 10.22075/JRCE.2020.13379.1243

[30] Vailati, M., Monti, G. (2016). "Earthquake-resistant and thermo-insulating infill panel with recycled-plastic joints." In Earthquakes and Their Impact on Society, pp. 417-432. doi: 10.1007/978-3-319-21753-6_15

[31] Markulak, D., Dokšanović, T., Radić, I., Miličević, I. (2018). "Structurally and environmentally favorable masonry units for infilled frames." Engineering Structures, 175, pp.753-764. doi. /10.1016/j.engstruct.2018.08.073

[32] Hosseini-Gelekolai, S.M., & Tabeshpour, M. (2011). Soft story design in reinforced concrete structure and effect of masonry infill wall. In Proceedings, sixth international conference of seismology and earthquake engineering, CDROM Tehran, Iran (pp. 1-18).

[33] Tsantilis, A.V., Triantafillou, T.C. (2020). "Innovative Seismic Isolation of Masonry Infills in Steel Frames using Cellular Materials at the Frame-Infill Interface." Journal of Earthquake Engineering, Vol. 24, pp. 1729–1746.

doi: 10.1080/13632469.2018.1478347

[34] Specification for structural steel buildings (ANSI/AISC 360-10)

[35] Flanagan, R.D., Bennett, R.M. (1999). "Bidirectional Behavior of Structural Clay Tile Infilled Frames." Journal of structural engineering, Vol. 125, pp. 236–244. doi: 10.1061/(ASCE)0733-9445(1999)125:3(236)

[36] Bennett, R.M.; Boyd, K.A.; Flanagan, R.D. (1997). "Compressive Properties of Structural Clay Tile Prisms." Journal of structural engineering, Vol. 123, pp. 920–926. doi: 10.1061/(ASCE)0733-9445(1997)123:7(920)

[37] Tsantilis, A.V., Triantafillou, T.C. (2018). "Innovative seismic isolation of masonry infills using cellular materials at the interface with the surrounding RC frames." Engineering Structures. Vol. 155, pp. 279–297. doi: 10.1016/j.engstruct.2017.11.025

[38] Rahmani, O., Adami, S.H. (2015). "Experimental study of static behavior of sandwich structures under flexural loading." 16th Marine Industry Conference, Bandar Abbas."In Persian"

[39] Ju, J., Kim, D.M., Kim, K. (2012). "Flexible cellular solid spokes of a non-pneumatic tire." Composite Structures, Vol. 94, pp. 2285–2295.

doi: 10.1016/j.compstruct.2011.12.022

[40] Schwarz, S., Hanaor, A., Yankelevsky, D.Z. (2015). "Experimental Response of Reinforced Concrete Frames With AAC Masonry Infill Walls to In-plane Cyclic Loading." Structures, pp. 306–319. doi: 10.1016/j.istruc.2015.06.005

[41] Abbasnejadfard, M., Farzam, M. (2016). "The effect of opening on stiffness and strength of infilled steel frames." Journal of Rehabilitation in Civil Engineering, Vol. 4, Issue 1, pp. 78-90. doi: 10.22075/JRCE.2016.494